blood.[16,17] We reported previously that HbV suspended in plasma-derived HSA or rHSA was almost Newtonian: no aggregation was detected microscopically.[3,18] In Japan, rHSA will soon be approved for clinical use.[19] However, various plasma substitutes such as hydroxylethyl starch (HES), dextran (DEX), and modified fluid gelatin (MFG) are used worldwide.[20−22] The selection among these plasma substitutes should be determined not only by safety and efficacy but also by price, experience of clinicians, and customs of respective countries.

Water-soluble polymers generally interact with particles such as polystyrene beads, silica, liposomes, and red blood cells (RBCs) to induce aggregation or flocculation.[23−28] For that reason, it is important to determine the compatibility of HbV with these plasma substitutes. With that background, we studied the rheological properties of HbV suspended in these plasma substitute solutions for the first time using a complex rheometer and a microchannel array. This study provides a unique opportunity to investigate the rheology of a highly concentrated liposomal suspension.

Materials and Methods

Preparation of HbV. The HbV used for this study was prepared by Oxygenix Co. Ltd. (Tokyo) under sterile conditions, as reported previously.[29−31] The Hb was purified from outdated donated blood provided by the Japanese Red Cross Society (Tokyo, Japan). The encapsulated purified Hb (38 g/dL) contained 14.7 mM pyridoxal 5′-phosphate (PLP; Sigma) as an allosteric effector at a molar ratio of PLP/Hb = 2.5. The lipid bilayer comprised a mixture of 1,2-dipalmitoyl-*sn*-glycero-3-phosphatidylcholine, cholesterol, and 1,5-bis-*O*-hexadecyl-*N*-succinyl-L-glutamate in a molar ratio of 5/5/1 (Nippon Fine Chemical Co. Ltd., Osaka, Japan) and 1,2-distearoyl-*sn*-glycero-3-phosphatidylethanolamine-*N*-poly(ethylene glycol) (NOF Corp., Tokyo, Japan, 0.3 mol % of the total lipid). The particle diameter was 279 ± 95 nm. The HbVs were suspended in a physiologic saline solution at [Hb] = 10 g/dL ([lipids] = ca. 6 g/dL) and were deoxygenated for storage with N_2 bubbling in vials.[32]

Plasma Substitutes. The plasma substitutes used in this study are listed in Table 1. Recombinant human serum albumin (rHSA, M_w = 67 kDa, 25 wt %) was a gift from Nipro Corp. (Osaka, Japan). Before use, it was diluted to 5 wt % using saline solution (Otsuka Pharmaceutical Co. Ltd., Osaka, Japan). DEX solution (M_w = 40 kDa, 10 wt % in a physiological saline solution) was purchased from Kobayashi Pharmaceutical Co. Ltd. (Osaka, Japan). An HES_{70} solution (Saline-HES, M_w = 68 kDa, 6 wt % in a physiological saline solution) was purchased from Kyorin Pharmaceutical Co. Ltd. (Osaka, Japan). An HES_{130} solution (Voluven, M_w = 130 kDa, 6 wt % in a physiological saline solution) and powdered HES_{200} (HES200/0.5, M_w = 200 kDa) were gifts from Fresenius Kabi AG (Homburg v.d.H., Germany). The HES_{200} was dissolved in a physiological saline solution at 6 wt %. An HES_{670} solution (Hextend, M_w = 670 kDa, 6 wt % in a physiological Ringer lactate solution) was obtained from Hospira, Inc. (Lake Forest, IL). An MFG solution (Gelofusin, M_w = 30 kDa, 4 wt % in a physiological saline solution) was a gift from B. Braun Melsungen AG (Melsungen, Germany). The COP was measured using a colloid osmometer (model 4420; Wescor, Inc., Logan, UT; molecular weight cutoff = 10 000).

Table 1. Plasma-Substitute Solutions and Their Physicochemical Properties[a]

plasma-substitute solutions	M_w (kDa)	M_n (kDa)	M_w/M_n	conc (g/dL) in saline	COP (Torr)	viscosity (mPa·s) at 25 °C: at 10 s^{-1}	viscosity (mPa·s) at 25 °C: at 1000 s^{-1}
DEX	40[b]	25[b]	1.6	10[b]	44	4.5	4.5
MFG	30[b]	23[b]	1.3	4[b]	44	2.2	2.3
HES_{670}	670[b]	194[c]	3.5	6[b]	27	4.5	4.4
HES_{200}	240[b]	70[b]	3.4	6	29	2.5	2.5
HES_{130}	130[b]	50[b]	2.6	6[b]	35	2.3	2.3
HES_{70}	68[b]	17[b]	4.0	6[b]	34	2.0	2.0
rHSA	67[b]	67[b]	1.0	5	19	1.3	1.2

[a] The viscosities at 10 and 1000 s^{-1} are almost identical, indicating that these polymer solutions are Newtonian fluids. (See Supporting Information). DEX, dextran; HES, hydroxyethyl starch; MFG, modified fluid gelatin; rHSA, recombinant human serum albumin; COP, colloid osmotic pressure. [b] Data provided by the manufacturer. [c] Calculated from the concentration dependence of COP (unpublished data).

Preparation of HbV Suspended in Plasma Substitutes and Blood Samples. HbV suspended in a saline solution was ultracentrifuged (20 000*g*, 30 min) to produce HbV−particle sediment. After the removal of the upper saline solution, a plasma substitute solution was added, and the HbV was redispersed by stirring and vortexing; the final concentration was adjusted to [Hb] = 10 g/dL. Flocculation of HbV was apparent because HbV tended to phase separate and precipitate gradually when HbV was suspended either in HES_{670}, HES_{200}, HES_{130}, DEX, or MFG. However, the supernatant was transparent and not colored. Before rheological measurements, we measured the particle diameters using a light-scattering method (PCS submicron particle analyzer; Beckman Coulter Inc.) after diluting the flocculated HbV with a normal saline solution. The particle diameters (nm) of redispersed HbV (HbV-DEX, 270 ± 81; HbV-HES_{670}, 292 ± 101; and HbV-MFG, 278 ± 90) were almost identical to that of the original HbV suspension (279 ± 95 nm). These results indicate that no hemolysis occurred and that no morphological change in the individual HbV particles occurred. Immediately before measurement, the suspension was filtered (0.45 μm pore size, Dismic; Toyo Roshi Kaisha Ltd., Tokyo, Japan). For comparison, fresh human blood was withdrawn with heparinized syringes from three donors. Measurements were performed within 6 h after withdrawal.

Viscoelastic Measurement of HbV Suspended in Plasma Substitutes. Steady-shear viscosity and shear stress measurements, a strain−sweep measurement, and the step-shear rate procedure (relaxation test) were performed using a rheometer (Physica MCR 301; Anton Paar GmbH, Graz, Austria). The cone diameter was 50 mm; the gap angle between the cone and plate was 1°. A parallel plate (50 mm diameter) was also used to confirm the influence of the interface between the plates and the test materials. All measurements were performed at 25 °C. About 650 μL of the sample suspension was sandwiched between the cone and plate. The excess solution was wiped out. For the steady-shear viscosity measurement, the shear rate was decreased from 10^3 to 10^{-4} s^{-1}. The shear rate was increased from 10^{-4} to 10^3 s^{-1} to confirm the presence of dynamic hysteresis. In this case, a preconditioning operation was performed for 60 s at 1 s^{-1} and then standing still for 300 s. Some variance in the data was apparent at a lower shear rate, and the averaged viscosities and standard deviations are shown with the data (n = 3).

(16) Sakai, H.; Masada, Y.; Horinouchi, H.; Yamamoto, M.; Ikeda, E.; Takeoka, S.; Kobayashi, K.; Tsuchida, E. *Crit. Care Med.* **2004**, *32*, 539−545.
(17) Yamazaki, M.; Aeba, R.; Yozu, R.; Kobayashi, K. *Circulation* **2006**, *114*, I220−I225.
(18) Sakai, H.; Tsai, A. G.; Kerger, H.; Park, S. I.; Takeoka, S.; Nishide, H.; Tsuchida, E.; Intaglietta, M. *J. Biomed. Mater. Res.* **1998**, *40*, 66−78.
(19) Kobayashi, K. *Biologicals* **2006**, *34*, 55−59.
(20) Webb, A. R.; Nash, G. B.; Dormandy, J. A.; Bennett, E. D. *Clin. Hemorheol.* **1990**, *10*, 287−296.
(21) Webb, A. R.; Barclay, S. A.; Bennett, E. D. *Intensive Care Med.* **1989**, *15*, 116−120.
(22) Traylor, R. J.; Pearl, R. G. *Anesth. Analg.* **1996**, *83*, 209−212.
(23) Meyuhas, D.; Nir, S.; Lichtenberg, D. *Biophys. J.* **1996**, *71*, 2602−2612.
(24) Sunamoto, J.; Iwamoto, K.; Kondo, H. *Biochem. Biophys. Res. Commun.* **1980**, *94*, 1367−1373.
(25) Otsubo, Y. *Langmuir* **1990**, *6*, 114−118.
(26) Tilcock, C. P.; Fisher, D. *Biochim. Biophys. Acta* **1982**, *688*, 645−652.
(27) Neu, B.; Meiselman, H. J. *Biophys. J.* **2002**, *83*, 2482−2490.
(28) Goto, Y.; Sakakura, S.; Hatta, M.; Sugiura, Y.; Kato, T. *Acta Anaesthesiol. Scand.* **1985**, *29*, 217−223.
(29) Takeoka, S.; Ohgushi, T.; Terase, K.; Ohmori, T.; Tsuchida, E. *Langmuir* **1996**, *12*, 1755−1759.
(30) Sou, K.; Naito, Y.; Endo, T.; Takeoka, S.; Tsuchida, E. *Biotechnol. Prog.* **2003**, *19*, 1547−1552.
(31) Sakai, H.; Masada, Y.; Takeoka, S.; Tsuchida, E. *J. Biochem. (Tokyo)* **2002**, *131*, 611−617.
(32) Sakai, H.; Tomiyama, K.; Sou, K.; Takeoka, S.; Tsuchida, E. *Bioconjugate Chem.* **2000**, *11*, 425−432.

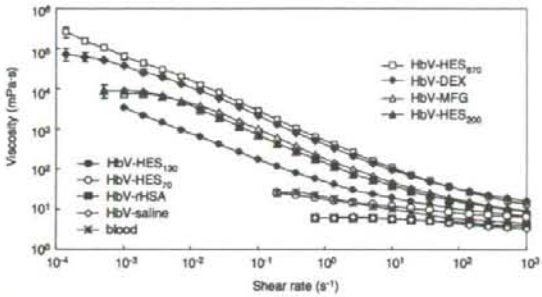

Figure 1. Viscosity of HbV suspended in various plasma-substitute solutions measured using an MCR 301 rheometer. The shear rate was decreased from 10^3 to 10^{-4} s^{-1}. Fluids with higher viscosity were measurable at a lower shear rate because of a sufficiently high strain of detection. Therefore, the low-viscosity HbV-rHSA and HbV-saline were measurable only above 0.7 s^{-1}. [Hb] = 10 g/dL, 25 °C. The blood data are inserted for comparison. Mean ± SD (n = 3).

Strain-sweep measurements were carried out in the strain range of 0.01−100% at a frequency of 2 Hz using the same cone-and-plate geometry.

For the step-shear rate procedure, the viscosity of the HbV suspension was measured continuously for 120 s at a shear rate of 0.1 s^{-1} to confirm the constant viscosity. Next, the rotation speed of the cone plate was increased suddenly to attain a shear rate of 100 s^{-1}; this condition was maintained for 220 s. Subsequently, the rotational speed was lowered suddenly to attain a shear rate of 0.1 s^{-1}; this condition was maintained for 20 s. The response of the viscosity to the stepwise change of shear rates reflects the morphological change of HbV flocculation.

The respective dependencies of the storage modulus (G'), loss modulus (G''), and complex viscosity on the shear rate were analyzed using a dynamic capillary rheometer (DCR; Anton Paar GmbH) at shear rates of 5−330 s^{-1} at 37 °C.[33]

Microchannel Flow Measurement. An array of microchannels (4.5 μm deep, 7 μm wide, 30 μm long, number 8736 in parallel, Bloody 6-7; Hitachi Haramachi Electronics Co. Ltd.) was used.[34] It was installed in a microchannel array flow analyzer (MC-FAN; Hitachi Haramachi Electronics Co. Ltd.). About 200 μL of the sample solution was inserted into the inlet syringe in order to flow through the microchannel array. The time necessary for a 100 μL suspension to pass through the channels at 20 cmH_2O, which corresponds to the capillary perfusion pressure, was measured (n = 3). Microscopic images were made of the flow patterns and the flocculate formation under a static condition (shutoff).

Results

Viscosity and Shear Stress of HbV Suspended in Plasma Substitutes. Figure 1 shows the viscosity of HbV suspended in various plasma substitute solutions when the shear rate decreased from 10^3 to 10^{-4} s^{-1}. The HbV suspended in rHSA was a nearly Newtonian fluid; no remarkable difference existed between HbV-rHSA and HbV suspended in saline. The respective viscosities of HbV-rHSA and HbV-HES_{70} were nearly equal to those of human blood in comparison with other combinations. Because of the detection limit of shear strain of this rheometer and the very low viscosity of HbV-rHSA, only measurements above 5 × 10^{-1} s^{-1} were valid. However, HbV suspended in other polymer solutions—HES, DEX, and MFG—showed non-Newtonian properties with a high viscosity at lower shear rates, so-called

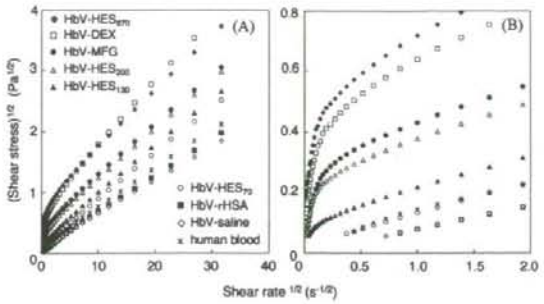

Figure 2. Casson plots of the square root of shear stress versus the square root of shear rate. These lines indicate that no clear stress yield exists. The graph is magnified in part B. Blood data are inserted for comparison.

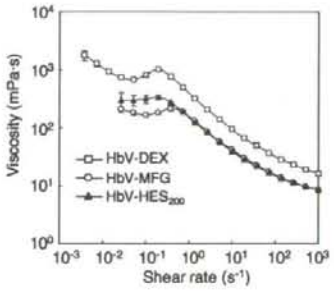

Figure 3. Shear thickening of HbV-DEX, HbV-HES_{200}, and HbV-MFG observed when the shear rate was increased in the opposite direction, from 10^{-4} to 10^3 s^{-1}. [Hb] = 10 g/dL, 25 °C. Mean ± SD (n = 3).

shear-thinning, attributable to the flocculate formation of HbV. The viscosities were measurable over a wider range of shear rates.

The series of different molecular weights of HES for HbV-HES reflected the molecular weight dependence of the viscosity: higher-molecular-weight HES displayed enhanced HbV flocculation.

As a comparative study, the shear rate dependencies of the viscosities of all of the plasma substitute solutions were measured. All solutions showed constant viscosities, indicating that they are all Newtonian fluids,[35−37] as shown in Table 1 and in Supporting Information.

Figure 2A,B shows Casson plots of shear stress versus the shear rate for all suspensions. HbV suspended in saline, rHSA, and HES_{70} showed a relatively linear relationship. Other suspensions with high viscosities showed convex curves with marked deviations from the linear relationship, especially at lower shear rates. No stress yield is apparent for any line, even when the graph is magnified (Figure 2B).

Suspensions of HbV-DEX, HbV-HES_{200}, and HbV-MFG showed hysteresis of viscosity at lower shear rates (Figure 3) when the shear rate was changed in the opposite direction, from 10^{-4} to 10^3 s^{-1}. In addition, a shoulder or a peak was visible at

(33) Thurston, G. B. *Biophys. J.* **1972**, *12*, 1205−1217.
(34) Kikuchi, Y.; Sato, K.; Mizuguchi, Y. *Microvasc. Res.* **1994**, *47*, 126−139.
(35) Tirtaatmadja, V.; Dunstan, D. E.; Boger, D. V. *J. Non-Newtonian Fluid Mech.* **2001**, *97*, 295−301.
(36) Cory, W. D.; Jackson, L. J.; Seaman, G. V. *Biorheology* **1983**, *20*, 705−717.
(37) Wulansari, R.; Mitchell, J. R.; Blanhard, J. M. V.; Paterson, J. L. *Food Hydrocolloids* **1998**, *12*, 245−249.
(38) Buscall, R.; Mills, P. D. A.; Goodwin, J. W.; Lawson, D. W. *J. Chem. Soc., Faraday Trans. 1* **1988**, *84*, 4249−4260.
(39) Chen, M.; Russel, W. B. *J. Colloid Interface Sci.* **1991**, *141*, 564−577.

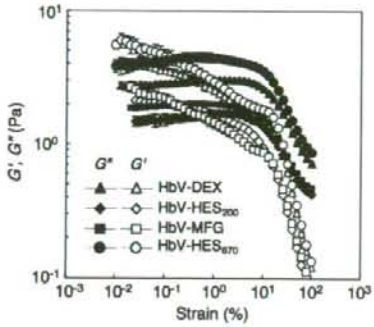

Figure 4. Strain dependence of the storage modulus (G') and loss modulus (G'') of HbV suspended in various plasma substitutes. [Hb] = 10 g/dL, f = 2 Hz. Mean ± SD (n = 3).

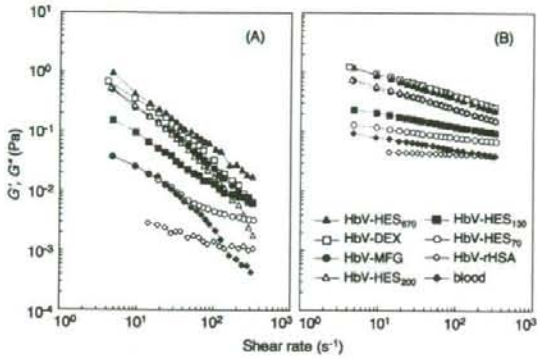

Figure 5. Respective shear rate dependencies of (A) the storage modulus, G', and (B) the loss modulus, G'', of HbV suspended in various plasma-substitute solutions as measured using a DCR rheometer. [Hb] = 10 g/dL, 37 °C. The blood curves are shown for comparison.

around 0.1−1 s^{-1}, indicating the presence of shear thickening in this range. However, suspensions with lower viscosities—HbV-HES_{70} and HbV-HES_{130}—showed a monotonous shear-thinning viscosity change (data not shown). Measurements with the parallel plate at different thicknesses of the suspensions also showed the shear-thickening effect (data not shown), indicating that this phenomenon is reproducible and unrelated to a skidding effect at the interface of the plate and the suspension.

Measurement of the Storage Modulus (G') and Loss Modulus (G''). Figure 4 shows the strain dependence of the storage modulus (G') and loss modulus (G'') at [Hb] = 10 g/dL, f = 2 Hz. The elastic responses were predominant, producing higher G' values than G'' values at lower strains for the highly flocculated HbV suspensions: HbV-DEX, HbV-HES_{670}, HbV-HES_{200}, and HES-MFG. The G' value decreased gradually with increasing strain, but G'' was nearly constant at lower strains. Yielding points (critical strain γ_c) for these suspensions were at around 10% strain; in addition, the γ_c values for the three samples were almost identical, irrespective of the different levels of G''. For HbV-rHSA, both G' and G'' were too small to detect and were therefore not included in the Figure.

Figure 5 shows the shear rate dependency of G' and G'' as measured using the capillary rheometer. At a lower shear rate, highly flocculated HbV suspensions HbV-DEX, HES_{670}-HbV, HbV-HES_{200}, and HbV-MFG showed high G' values. The contribution of G' decreased considerably when the HbV concentration was reduced at a constant polymer concentration.

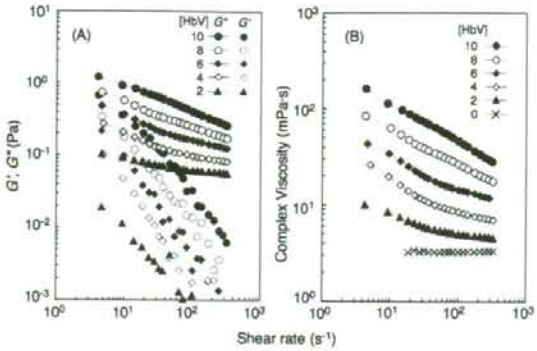

Figure 6. Representative profile of the concentration dependence (A) on G' and G'' and (B) on complex viscosity when the concentration of HbV in HbV-DEX was reduced from [Hb] = 10 to 0 g/dL at a constant DEX concentration (10 g/dL).

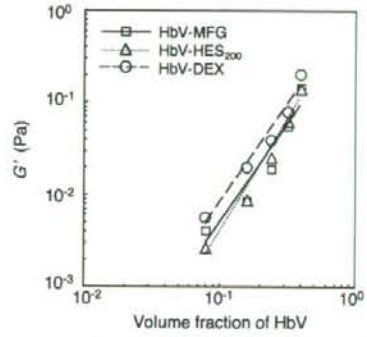

Figure 7. Logarithmic plots of G' at 18 s^{-1} vs ϕ (volume fraction of HbV) for HbV-DEX, HbV-HES_{200}, and HbV-MFG. For all cases, G' varies with ϕ following a power law of order 2.1−2.4. HbV-DEX, $G'-\phi^{2.13}$ (R^2 = 0.9722); HbV-HES, $G'-\phi^{2.45}$ (R^2 = 0.9753); and HbV-MFG, $G'-\phi^{2.14}$ (R^2 = 0.9139).

Figure 6A shows a representative profile of HbV-DEX at a constant dextran concentration. The complex viscosity of HbV-DEX depends strongly on the concentration of HbV (**Figure 6B**). For example, the complex viscosity at 320 s^{-1} decreased from 28 to 5 mPa·s when the Hb concentration decreased from 10 to 2 g/dL. Other plasma substitutes displayed similar profiles (data not shown).

The relationship between G' and ϕ (volume fraction of HbV) provides important information about the nature of particle flocculation.[35,36] Figure 7 shows a logarithmic graph of G' at 18 s^{-1} versus ϕ for HbV-DEX, HbV-HES_{200}, and HbV-MFG. Those graphs show an almost linear relationship: G' varies with ϕ, following a power law of order 2.1−2.4.

Relaxation Test of HbV Suspended in Plasma Substitutes. Figure 8A shows the response of viscosity to the rapid change of the shear rate. At a low shear rate (0.1 s^{-1}), the suspensions of HbV-DEX, HbV-HES_{670}, HbV-HES_{200}, and HbV-MFG showed very high viscosities because of flocculation. The viscosities decreased rapidly when the shear rate increased rapidly to 100 s^{-1} (which corresponds to the shear rate in a venule). The viscosities returned spontaneously to the original levels when the shear rate reverted rapidly to 0.1 s^{-1}. Figure 8B shows a magnification of the data for jumping points of Figure 8A, which clarifies that the suspension responded very promptly to the change in the shear rate. The reduction of viscosities that corresponded to the dissociation of flocculation was completed within 0.2 s,

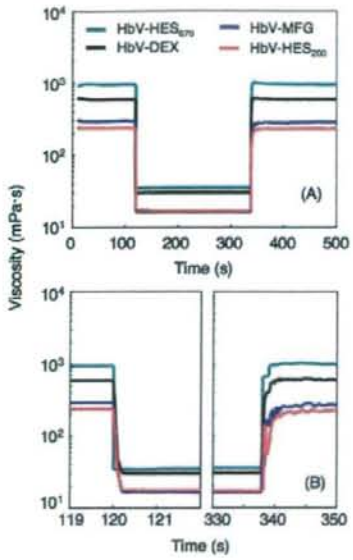

Figure 8. (A) Response of the viscosity of HbV suspended in DEX, HES_{200}, HES_{670}, and MFG to the rapid change in shear rate as measured using the MCR 301 rheometer. The shear rate changed rapidly from 0.1 to 100 s^{-1}; it then returned to 0.1 s^{-1}. The graph is magnified in B. [Hb] = 10 g/dL, 25 °C.

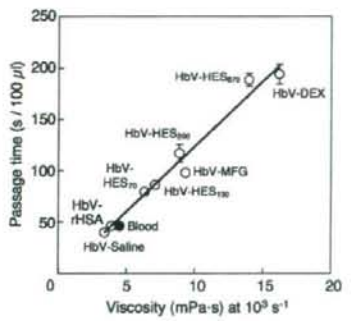

Figure 9. Microchannel flow measurements of HbV suspended in various plasma-substitute solutions and human blood. The time required for the passage of 100 μL of each suspension was plotted against the viscosity at 1000 s^{-1} (from Figure 1). The straight line indicates a linear approximation: $Y = 12.4X$ ($R^2 = 0.9727$). Mean ± SD ($n = 3$).

and the recovery of viscosity that corresponded to flocculate formation was completed within 2 s. Although the responses should depend partially on the sharpness of the shear rate change induced by the motion of the cone plate, these data indicate that the flocculation of HbV is formed rapidly by weak interaction and that it is completely reversible.

Microchannel Flow Measurement. Figure 9 summarizes the relationship between the viscosity of the HbV suspensions at a shear rate of 10^3 s^{-1} and the time required for the passage of 100 μL of the suspensions through the microchannels. The most viscous HbV-DEX required the longest time: 194 ± 10 s. Apparently, a proportional relationship exists between the time required for passage and the fluid viscosity ($R^2 = 0.9727$).

Despite the high viscosities of HbV-DEX, HbV-HES_{670}, HbV-MFG, and HbV-HES_{200}, microscopic observation indicated that no plugging of the microchannels occurred under the flow

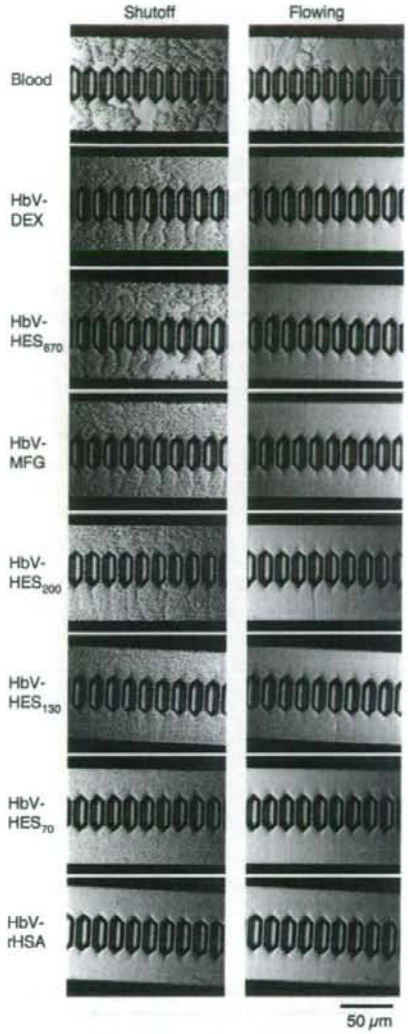

Figure 10. Images of microchannels during the flowing condition and at flow cessation. The direction of flow is from top to bottom. Flocculate formation is apparent at cessation for HbV-DEX, HbV-HES, and HbV-MFG. However, no flocculation was apparent for HbV-rHSA. Under the flowing condition, no plugging of channels occurred for any HbV suspension. However, blood showed partial plugging. In the HES series, a higher-molecular-weight HES shows larger flocculation at cessation.

condition even though clear flocculate formation existed for the cessation of flow (Figure 10). However, stored blood showed the partial plugging of channels even though its viscosity (4.5 mPa·s) and the time required for passage (48 s) were much less than that for HbV suspended in other polymer solutions. At shutoff, HbV-DEX, HbV-MFG, HbV-HES_{200}, and HbV-HES_{670} showed traces of channel flow and phase separation of the suspending medium and flocculation.

Discussion

The results of this study clarified that the HbV suspension has a unique rheological profile from the viewpoint of "suspension rheology." Liposomes are well known to form flocculates or

aggregates in the presence of water-soluble polymers[23,24,40] that were analyzed mainly by turbidity or light-scattering measurements at a very low concentration, where a suspension would consist of a collection of discrete flocculates. However, the HbV suspension consists of a high concentration of HbV with a weight fraction of nearly 16 g/dL in all and a volume fraction of about 40 vol %. Therefore, the flocculated HbV would respond elastically to small deformations, as indicated by the considerable increase in the storage modulus (G') of flocculated suspensions.[25,41] The rheometer that we used (Physica MCR 301) is extremely sensitive to slight shear stress, thereby enabling the detection of subtle rheological changes over a wide range of shear rates (10^{-4}–10^{3} s^{-1}). The RBCs are well known to aggregate reversibly; they are a determinant of the viscoelastic property of non-Newtonian blood because they occupy 40–55% of the blood volume.[33,42] The RBC aggregation, induced by the addition of a water-soluble polymer, influences blood viscosity, hemodynamics, and tissue oxygenation.[43–46] Therefore, it is important to determine the rheological profiles of HbV suspensions as a transfusion alternative.

The HbV suspended in rHSA, a globular protein solution, was a nearly Newtonian fluid. The level of viscosity at higher shear rates was nearly equal to that of human blood. In contrast, HbV suspended in other polymer solutions—HES, DEX, and MFG—showed non-Newtonian properties with a high viscosity at a lower shear rate (shear thinning) because of the flocculation of HbV. A series of HES solutions showed a clear molecular-weight dependence for inducing flocculation. In addition, HbV-HES_{70} showed a similar curve to that of blood. For all combinations of HbV and a polymer solution, the flocculation of HbV should be dissociated at a higher shear rate. Interestingly, the Casson plots show no stress yield for any suspension, probably because the rheometer that we used can measure shear stress values successively, even at extremely low shear rates of 10^{-4} s^{-1}. It is speculated that flocculation formation and dissociation are successive and that no marked critical point exists.

The mechanism of liposome flocculation remains controversial. It is well established in our laboratory that intermacromolecular interactions in water solutions produce macromolecular complexes such as a polyelectrolyte complex and a hydrogen-bonding complex.[47] Therefore, it was plausible that (i) polymer chains would adsorb onto the surfaces of the particles directly to produce bridges.[24] However, it is well known that a PEG aqueous solution and a polysaccharide aqueous solution are immiscible, and it cannot explain the adsorption of DEX and HES on the surface of PEG-modified HbV. Another mechanism was that (ii) the hydration of polymer chains would deflect water molecules from the particles and thereby exclude the particles from the bulk solution.[26] However, this was denied by Meyuhas et al.[23] by the fact that dialysis of liposomes against polymer-containing solutions did not induce aggregation whereas direct addition of the polymer to the liposome solution induced flocculation. Recent practical and theoretical analyses contradict these theories and suggest a depletion mechanism: (iii) A depletion layer develops near a particle surface that is in contact with a polymer solution if the loss of configurational entropy of the polymer coil is not balanced by adsorption energy. Within this layer, the polymer concentration is lower than in the bulk phase. Consequently, as particles approach, the osmotic pressure difference between the interparticle polymer-poor depletion layer and the bulk phase results in solvent displacement into the bulk phase and depletion interaction. Because of this interaction, an attractive force of particles tends to minimize the polymer-poor space between the particles, thereby inducing flocculation.[23,27,48,49]

In the case of depletion interaction, the size of the polymer coil in comparison to interparticle spacing is important. Macromolecules of HES, DEX, and MFG should contain branches; the polymers are more extended or linear than the globular, compact structure of HSA.[50] According to the literature, the radii of gyration (R_g) of these polymers are estimated to be HES_{670} (ca. 19.7 nm), HES_{130} (ca. 12.3 nm),[51] DEX (ca. 8.1 nm),[52] MFG (ca. 10.7 nm),[53] and HSA with the smallest value (ca. 2.8 nm).[54] Even though the R_g of MFG is only half that of HES_{670}, the molar concentration of MFG (1.7 mM), calculated from the concentration and M_n, is about 6 times larger than that of HES_{670} (0.3 mM). It is probable that the more extended polymer chains and the higher molar concentration enhance the exclusion effect from the hydrated sphere of the vesicles, creating a more flocculated vesicle structure. One limitation of this study is that we selected the clinically approved polymer solutions only from a practical point of view. Therefore, the molecular weight distributions are very wide, as indicated by their large M_w/M_n ratios, and their molar concentrations are different. Further analyses are ongoing to clarify the flocculation mechanism using polymers with strictly defined molecular weights and concentrations.

Interestingly, we observed dynamic hysteresis and a shear-thickening profile when the shear rate was increased in the opposite direction for suspensions that showed very high viscosities (HbV-DEX, HbV-HES_{670}, HbV-HES_{200}, and HbV-MFG). These results indicate that the rheological properties of these suspensions are influenced by the time history of the suspension for the growth of flocculation. Typical shear thickening is reported in the case of styrene-methyl acrylate copolymer particles mixed with poly(acrylic acid),[55] which is attributable to the nonlinear elasticity resulting from the entropy of extended bridges and forced desorption caused by hydrodynamic effects. For HbV suspensions, it is speculated that a higher shear rate would extend the distance separating the HbV particles, causing an entropy loss of the solution of polymers with larger R_g, which would cause a regional shear-thickening effect. Another reason would be related to the sedimentation of flocculated HbV, even in the thin solution between the cone and plate. In this case, the concentration of HbV would be lower at the upper layer near the cone, resulting in a slightly lower viscosity at a lower shear rate. With increasing shear rate, the suspension would be homogenized, showing a higher viscosity as a shoulder in Figure 3.

(40) Sou, K.; Endo, T.; Takeoka, S.; Tsuchida, E. *Bioconjugate Chem.* **2000**, *11*, 372–379.
(41) Otsubo, Y. *Heterogeneous Chem. Rev.* **1996**, *3*, 327–349.
(42) Chien, S.; King, R. G.; Skalak, R.; Usami, S.; Copley, A. L. *Biorheology* **1975**, *12*, 341–346.
(43) Freyburger, G.; Dubreuil, M.; Boisseau, M. R.; Janvier, G. *Br. J. Anaesth.* **1996**, *76*, 519–525.
(44) Eckmann, D. M.; Bowers, S.; Stecker, M.; Cheung, A. T. *Anesth. Analg.* **2000**, *91*, 539–545.
(45) Bishop, J. J.; Nance, P. R.; Popel, A. S.; Intaglietta, M.; Johnson, P. C. *Am. J. Physiol. Heart Circ. Physiol.* **2001**, *280*, H222–H236.
(46) Tateishi, N.; Suzuki, Y.; Cicha, I.; Maeda, N. *Am. J. Physiol. Heart Circ. Physiol.* **2001**, *281*, H448–H456.
(47) Tsuchida, E.; Abe, K. *Adv. Polym. Sci.* **1982**, *45*, 1–119.
(48) Neu, B.; Meiselman, H. J. *Biochim. Biophys. Acta* **2006**, *1760*, 1772–1779.
(49) Vincent, B.; Edwards, J.; Emmett, S.; Jones, A. *Colloids Surf.* **1986**, *18*, 261–281.
(50) Takaori, M.; Kobori, M. *Plasma Substitutes and Their Clinical Use*; Kokuseido Publisher: Tokyo, 2004.
(51) Gosch, C. I.; Haase, T.; Wolf, B. A.; Kulicke, W. *Starch* **2002**, *54*, 375–384.
(52) Hirata, Y.; Sano, Y.; Aoki, M.; Shohji, H.; Katoh, S.; Abe, J.; Hitsukuri, S.; Yamamoto, H. *Carbohydr. Polym.* **2003**, *53*, 331–335.
(53) Kaur, M.; Jumel, K.; Hardie, K. R.; Hardman, A.; Meadows, J.; Melia, C. D. *J. Chromatogr., A* **2002**, *957*, 139–148.
(54) Almogren, A.; Furtado, P. B.; Sun, Z.; Perkins, S. J.; Kerr, M. A. *J. Mol. Biol.* **2006**, *356*, 413–431.
(55) Otsubo, Y. *Langmuir* **1999**, *15*, 1960–1965.

The elastic properties of the HbV suspension are readily apparent from the high contribution of the storage modulus (G'). In fact, G' was higher for more viscous HbV suspensions, such as HbV-DEX, HbV-HES_{200}, and HbV-MFG. The strain−sweep measurement clarified that G' decreased gradually with increasing strain. However, G'' was nearly constant at lower strains, and the yielding point for these suspensions was as high as 10% strain. These results indicate that the HbV flocculation structure is not rigid and that reformation occurs easily with subtle strain.

It is speculated that the flocculation of HbV includes interconnected fractal clusters. As shown in Figure 6, both G' and the viscosity increase with increasing concentration of HbV. The logarithmic graph of G' versus ϕ (volume fraction of HbV) shows an almost linear relationship. A theory of Bascall et al.[38] for networks consisting of interconnected fractal clusters predicts $G'-\phi^{3.5\pm0.2}$ for diffusion-limited flocculation and $G'-\phi^{4.5\pm0.2}$ for chemically limited aggregation.[39] For the HbV suspensions, G' varies with ϕ following a power law of order 2.1−2.4 and is much smaller than the theoretical values, supporting the idea that HbV forms fractal clusters through a very weak interaction and that diffusion-limited flocculation is plausible. This also supports the idea that polymer adsorption on the surface of HbV would not involve this system and that the weak interaction enables reversible and rapid flocculation−dissociation in response to the rapid change in shear rates, as shown in Figure 8, and the high yielding point of the stress−sweep measurement in Figure 4.

We reported previously that the surface modification of HbV with PEG prevents aggregation in an HSA solution.[3,18] The amount of PEG is sufficient to prevent aggregation formation in plasma. However, results of the present study show that, even with the PEG modification, HbV undergoes flocculation or aggregation when dispersed into a series of plasma substitutes. Notwithstanding, the flocculation seems not to plug the capillaries, as demonstrated for the first time by microchannel flow experiments. Under a static condition, microscopic observation clearly revealed flocculation. Under the flowing condition in the microchannels, visual observation confirmed the flocculation. However, no plugging was detected in the channels. The time necessary for passage at a perfusion pressure of 20 cmH_2O, which corresponded to an in vivo capillary pressure, was proportional to the fluid viscosity, according to Poiseuille's theory at constant pressure. However, the time required for the passage of blood should depend on the deformability of red blood cells and the activation of platelets and white cells, depending on a pathological condition.[34]

In a living body, perfusion pressure, vascular resistance, and blood viscosity determine organ blood flow. According to Poisseuille's law, increased viscosity reduces flow at a constant applied pressure. For the substitution of a large volume of blood with an HbV suspension as a "transfusion alternative", HbV-rHSA and HbV-HES_{70} with similar viscosity to that of human blood would apparently be appropriate to maintain blood rheology and systemic hemodynamics. It remains to be examined whether other viscous combinations of HbV with DEX, higher-molecular-weight HES, and MFG would be acceptable to a living body. A possible utilization of HbV would be injection at a perioperative hemorrhage. A plasma substitute solution would be injected in an initial phase to maintain blood volume, causing hemodilution, followed by the injection of HbV to maintain O_2 content. This procedure would cause the dilution of both the plasma substitute and HbV. Therefore, the level of HbV flocculation and the viscosity would be reduced somewhat. Actually, we conducted the isovolemic hemodilution of 60% blood volume of rats with the series of plasma substitute solutions and subsequent injection of HbV. The results showed that systemic hemodynamic and respiratory functions were preserved and that no effect of flocculation was evident (unpublished data). The details will be reported elsewhere.

From a physiological point of view, changes in blood viscosity are accompanied by changes in vascular geometry because of autoregulatory processes that are driven by changes in the production of endothelium-derived vasorelaxation factors such as nitric oxide and prostacyclin in response to shear stress on the vascular wall.[56] Progressive hemodilution with a plasma substitute solution decreases blood viscosity, thereby increasing blood flow and vasoconstriction.[57] However, a viscous fluid is advantageous for imparting shear stress on the vascular wall to facilitate the production of vasorelaxation factors and thereby enhance vasorelaxation to improve peripheral blood flow. High blood viscosity is advantageous for transmitting pressure homogeneously to the microvascular network and thereby supplying blood to all capillaries.[58−60] A high-molecular-weight dextran-induced hyperviscosity of blood engenders the dilation of blood vessels.[61] Hemoconcentration increases blood viscosity but reduces vascular resistance.[62] Actually, Erni et al. tested the 40% blood exchange transfusion with HbV suspended in DEX and HES_{200}; they found no capillary plugging. They did find increased plasma viscosity and an improvement of microcirculatory blood flow in ischemic tissues in a hamster skin-flap model.[63−65]

In conclusion, the rheological property of HbV suspension is adjustable to that of human blood through the combination of rHSA and HES_{70}. Other plasma substitutes, such as high-molecular-weight HES, DEX, and MFG, cause HbV flocculation and hyperviscosity. However, reports show that hyperviscosity would not necessarily cause deterioration and in some cases might be advantageous to the body. The combination of HbV and plasma substitute solutions provides a unique opportunity to manipulate the suspension rheology not only as a transfusion alternative but also for other clinical applications such as the oxygenation of ischemic tissues and the ex vivo perfusion system. Further research is necessary to clarify the mechanism of flocculation and the in vivo safety of the combination of HbV and various kinds of plasma substitutes. Projects to collect such data are under way.

Acknowledgment. We acknowledge Dr. Masuhiko Takaori (East Takarazuka Satoh Hospital), Dr. Amy G. Tsai (University of California, San Diego), and Dr. Dominique Erni (Inselspital Hospital, University of Bern) for meaningful discussions related to plasma substitutes and Professor Yasufumi Otsubo (Chiba University) and Mr. N. Hirano (Nihon SiberHegner K.K., Tokyo)

(56) Smiesko, V.; Johnson, P. C. *News Physiol. Sci.* **1993**, *8*, 34−38.
(57) Hudak, M. L.; Jones, M. D., Jr.; Popel, A. S.; Koehler, R. C.; Traystman, R. J.; Zeger, S. L. *Am. J. Physiol. Heart Circ. Physiol.* **1989**, *257*, H912−H917.
(58) Tsai, A. G.; Acero, C.; Nance, P. R.; Cabrales, P.; Frangos, J. A.; Buerk, D. G.; Intaglietta, M. *Am. J. Physiol. Heart Circ. Physiol.* **2005**, *288*, H1730−H1739.
(59) Tsai, A. G.; Intaglietta, M. *Biorheology* **2001**, *38*, 229−237.
(60) de Wit, C.; Schafer, C.; von Bismarck, P.; Bolz, S. S.; Pohl, U. *Pflugers Arch.* **1997**, *434*, 354−361.
(61) Chen, R. Y. Z.; Carlin, R. D.; Simchon, S.; Jan, K. M.; Chien, S. *Am. J. Physiol. Heart Circ. Physiol.* **1989**, *256*, H898−H905.
(62) Martini, J.; Tsai, A. G.; Cabrales, P.; Johnson, P. C.; Intaglietta, M. *Am. J. Physiol. Heart Circ. Physiol.* **2006**, *291*, H310−H317.
(63) Plock, J. A.; Contaldo, C.; Sakai, H.; Tsuchida, E.; Leunig, M.; Banic, A.; Menger, M. D.; Erni, D. *Am. J. Physiol. Heart Circ. Physiol.* **2005**, *289*, H2624−H2631.
(64) Contaldo, C.; Plock, J.; Sakai, H.; Takeoka, S.; Tsuchida, E.; Leunig, M.; Banic, A.; Erni, D. *Crit. Care Med.* **2005**, *33*, 806−812.
(65) Contaldo, C.; Schramm, S.; Wettstein, R.; Sakai, H.; Takeoka, S.; Tsuchida, E.; Leunig, M.; Banic, A.; Erni, D. *Am. J. Physiol. Heart Circ. Physiol.* **2003**, *285*, H1140−1147.

for discussions of technical problems pertaining to viscoelastic measurements. The rHSA, HES, and MFG used in this study were gifts from Nipro Co., Fresenius Kabi A.G., and B. Braun, respectively. This study was supported by Health and Labour Sciences Research Grants (Research on the Regulatory Science of Pharmaceuticals and Medical Devices), the Ministry of Health, Labour and Welfare, Japan (H.S., E.T.), Grants-in-Aid for Scientific Research from the Japan Society for the Promotion of Science (B16300162) (H.S.), and Oxygenix Inc. (Tokyo, Japan). H.S., S.T., and E.T. are consultants of Oxygenix Inc.

Supporting Information Available: Viscosity of plasma-substitute solutions. This material is available free of charge via the Internet at http://pubs.acs.org.

LA7004503

各種代用血漿剤に分散させたヘモグロビン小胞体(人工赤血球)とその血液混合系のレオロジー特性

佐藤 敦[1)]、酒井 宏水[2)]、武岡 真司[1)]、土田 英俊[*,2)]

[1)] 早稲田大学大学院 理工学研究科、[2)] 早稲田大学理工学術院 理工学研究所

【要旨】

ヘモグロビン小胞体(HbV)は、高濃度ヘモグロビン(Hb)溶液をリン脂質小胞体に内包した人工赤血球(人工酸素運搬体)である。HbV 分散液の膠質浸透圧は殆どゼロなので、大量投与に際しては代用血漿剤(水溶性高分子溶液)の併用が循環血液量の維持に重要となる。従来、ヒト血清アルブミン(HSA)或いはそのリコンビナント体(rHSA)を併用して、HbV の充分な酸素運搬効果と血行動態の維持を確認してきた。しかし、臨床現場ではアルブミン以外の代用血漿剤としてデキストラン(DEX)、ヒドロキシエチルスターチ(HES)、修正ゼラチン(MFG)などが使用されており、これらが HbV の分散安定性に及ぼす影響を検討する必要がある。これまで、各種代用血漿剤に分散させた HbV のレオロジー特性を詳細に検討してきたが、実際の投与では、代用血漿剤、HbV 分散液、そして血液が互いに希釈された混合系を形成する。そこで本研究では、各種代用血漿剤に分散させた HbV と血液の混合系のレオロジー特性、およびマイクロチャネルを通過する血液の流動性に HbV 凝集体が及ぼす影響を検討した。rHSA、低分子量 HES に分散させた HbV と血液の混合系は血液と同等あるいはそれ以下の粘度を示した。一方、DEX、高分子量 HES、MFG に分散させた HbV は血液よりも高い粘度を示したが、血液との混合比の増大に伴い、粘度および貯蔵弾性率の減少を示した。各種代用血漿剤に分散させた HbV と血液の混合液はマイクロチャネルを殆ど塞栓すること無く流動し、100 μL の通過時間は単純に粘度に比例した。HbV は可逆的な凝集性を示し、血液の微小流路の塞栓因子に影響を及ぼさないものと考えられる。HbV は分散媒である代用血漿剤との組み合わせでレオロジー特性を調節できるので、輸血代替以外の用途に拡大する可能性が期待できる。

【キーワード】 血液代替物、代用血漿剤、レオロジー

【緒言】

リン脂質小胞体（リポソーム）は薬剤を内包、或いは脂質膜に担持できる特徴を持つことから、ドラッグデリバリーシステムを目的とした精力的な研究が行われており、抗真菌療法や抗癌治療法として既に認可されている例もある[1)]。ヘモグロビン小胞体（HbV）は、高純度・高濃度ヒトヘモグロビン（Hb）をリン脂質小胞体（粒子径 280 nm）に内包した人工酸素運搬体である[2-5)]。これまでの動物投与試験から、HbV が血液と同等の酸素運搬能と十分な安全性を有することが明らかになっている。輸血代替としての投与量は非常に多く、循環血液量の 40 %以上になることも想定される。

受付日　2007/10/27　　受理日　2007/12/21

〒169-8555 東京都 新宿区 大久保 3-4-1
早稲田大学理工学術院 理工学研究所
TEL: 03-5286-3120
FAX: 03-3205-4740
E-mail: eishun@waseda.jp

赤血球と同等の酸素運搬機能を持たせるため、HbV 分散液の固形分濃度は他のリポソーム製剤と比較して非常に高い（Hb 濃度 10 g/dL; 脂質濃度 5〜6 g/dL）。

従って HbV の安全性を評価する上で、ヘモレオロジーに対比させて HbV 分散液のレオロジー特性を検討することは重要である[6)]。

血漿中に 5 g/dL 程存在するアルブミンは血液と間質液の膠質浸透圧（COP）を平衡に保ち、循環血液量を維持する機能を有する血漿蛋白質である。この機能を維持する為に、COP は血液代替物が備えるべき必須条件の一つである。HbV は 1 粒子あたり約 3 万個の Hb を内包しており、分散液の COP は殆どゼロである。従って、HbV の大量投与に際しては代用血漿剤の併用が循環血液量の維持に重要となる。従来、HbV を 5%アルブミン（HSA）溶液或いはリコンビナントアルブミン（rHSA）溶液に分散させ COP を 20 Torr に調節し、この分散液を用いた出血ショック蘇生試験や、循環血液量の 40〜90%を置換する試験から、rHSA に分散させた HbV が血液と同等の酸素運搬効果を有することを明らかにしてきた[7)]。HbV を rHSA に分散させて Hb 濃度を 8.6〜10 g/dL とした場合の粘度は血液と同等で

あり、剪断速度依存性からニュートン流体に近い挙動を示している[8]。しかし、実際の臨床現場ではHSA以外に代用血漿剤として、デキストラン（DEX）やヒドロキシエチルスターチ（HES）が使用されており、海外ではそれ以外に、HESの高分子量体や修正ゼラチン溶液（MFG）なども使用されている[9-11]。また、HbVをこれらの代用血漿剤に分散させて投与することで、虚血領域の酸素化の改善効果も報告されている[12-14]。このような背景のもと、我々は各種代用血漿剤に分散させたHbVのレオロジー特性の詳細な解析を進めている。rHSAと低分子量HESではHbVと混合しても顕著な粘度増大は見られないが、DEXおよび欧州や米国で使用されている高分子量HESやMFGではHbVの凝集生起を認め、粘度上昇が顕著となる。しかし凝集の形成と解離は極めて可逆的で迅速であり、血液流動性測定装置（Microchannel array flow analyzer, MC-FAN）[15, 16]のマイクロチャネルには一切の塞栓が無いことを確認している[8]。

代用血漿剤を静脈内投与した場合、血液と代用血漿剤の両方が希釈されるので、ここにHbV分散液が投与された場合、凝集形成は低減されると考えられる。また、HbVの凝集生起が血液の流動性に与える影響をin vitroで検討する必要がある。そこで本研究では、各種代用血漿剤に分散させたHbVと血液の混合系のレオロジー特性を観測すると共に、MC-FANを用いてHbVの凝集体が血液の流動性に及ぼす影響を明らかにすることを目的とした。

【方法】

1. HbV分散液の調製

HbV分散液は無菌条件下、既報に従って調製した[17-19]。Hb溶液は日本赤十字社（東京）から提供を受けた期限切れ非使用赤血球から精製した。HbVの内水相には高濃度のHb（38 g/dL）と共に、アロステリック因子としてピリドキサール5'-リン酸（PLP、14.7 mM）がモル比でPLP/Hb = 2.5になるように添加した。HbVの膜成分である脂質は、日本精化社製のPresome PPG-I（1,2–ジパルミトイル-*sn*-グリセロ-3-ホスファチジルコリン）、コレステロール、1,5-bis-*O*-ヘキサデシル-*N*-スクシニル-L-グルタメート = 5/5/1（モル比）に0.3 mol%の1,2-ジステアロイル-*sn*-グリセロ-3-ホスファチジルエタノールアミン-*N*-ポリ（エチレングリコール）（日本油脂社製）を混合して用いた。HbVは生理食塩水に分散、フィルター滅菌し（Dismic、東洋濾紙社製：0.45 μm）、窒素通気により酸素を除去して保存した[20]。HbVの粒子径は279 ± 95 nmであった。

2. 各種代用血漿剤

遺伝子組み換えヒト血清アルブミン（rHSA, Bipha, Mw. 67 kDa, 25 wt%溶液）は生理食塩水で5 wt%に希釈して用いた。デキストラン（DEX, 小林製薬工業 デキストラン40注「小林」™, Mw. 40 kDa, 10 wt%溶液）、低分子量ヒドロキシエチルスターチ（HES_{70}, 杏林製薬 サリンヘス™, Mw. 70 kDa, 6 wt %溶液）、中分子量ヒドロキシエチルスターチ（HES_{130}, HES_{200}, Fresenius社 Voluven™, Mw. 130 kDa, 200 kDa, 6 wt%溶液）、高分子量ヒドロキシエチルスターチ（HES_{670}, Hospira社 Hextend™, Mw. 670 kDa, 6 wt%溶液）、修正ゼラチン（MFG, B. Braun社 Gelofusine™, Mw. 30 kDa, 4 wt%溶液）を用いた。各種代用血漿剤の膠質浸透圧（COP）は浸透圧計（model 4420, Wescor社製、Cut-off Mw. = 10,000）を用いて測定した。物理化学的特徴は**Table 1**にまとめた。

Table 1. Plasma-substitute solutions and their physicochemical properties. The viscosities at 10 and 1000 s^{-1} are almost identical, indicating that these polymer solutions are Newtonian fluids.

Plasma Substitutes	Mw. (kDa)	Concentration (g/dL) in saline	COP (Torr)	Viscosity (mPa·s)	
				at 10 s^{-1}	at 1000 s^{-1}
DEX	40	10	44	4.5	4.5
MFG	30	4	44	2.2	2.3
HES_{670}	670	6	27	4.5	4.4
HES_{200}	200	6	29	2.5	2.5
HES_{130}	130	6	35	2.3	2.3
HES_{70}	70	6	34	2.0	2.0
rHSA	66.5	5	19	1.3	1.2

DEX, dextran; HES, hydroxyethyl starch; MFG, modified fluid gelatin; rHSA, recombinant human serum albumin; COP, colloid osmotic pressure.

3. 各種代用血漿剤に分散させたHbV及び血液試料の調製

生理食塩水に分散させたHbVを超遠心分離（20 000 g, 30 min）で沈降させて上澄みの生理食塩水を除去後、代用血漿剤中に分散させ（[Hb] = 10 g/dL）、フィルター処理した（Dismic、東洋濾紙社製：0.45 μm）。血液試料は5 %ヘパリン加ヒト新鮮血を用い、採血後6時間以内に測定を行った[21]。

4. 各種代用血漿剤に分散させたHbVとその血液混合系のレオロジー測定

粘度の剪断速度依存性はモジュラーコンパクトレオメータ（Physica MCR301 : Anton Paar社製）を用いて

測定した。測定治具はコーンプレート（コーン径：50 mm、ギャップ角度：1°）を用い、25 ℃で剪断速度を 10^3 から 10^{-4} s^{-1} に低下させた。動的粘弾性はキャピラリーレオメータ（DCR：Anton Paar 社製）を用いて測定した。キャピラリーレオメータでは、複素弾性率 G^* を測定できる。G^* は弾性項と粘性項に分けられ、弾性項（貯蔵弾性率 G'）は固体としての性質を、粘性項（損失弾性率 G''）は流体としての性質をそれぞれ示す。凝集体は弾性応答を示すので、貯蔵弾性率 G' の剪断速度依存性を測定した（剪断速度 5 ～ 320 s^{-1}、周波数 2 Hz、37 ℃）。

5. 各種代用血漿剤に分散させた HbV とその血液混合系のマイクロチャネル流動性試験

各種代用血漿剤に分散させた HbV（[Hb] = 10 g/dL）とヘパリン加ヒト新鮮血の混合液を測定試料とした。マイクロチャネルアレイ Bloody6-7（幅 7 μm, 長さ 30 μm, 深さ 4.5 μm, 流路数 8,736 本：日立原町電子工業社製）に MC-FAN（KH-3：日立原町電子工業社製）を用いて 20 cm 水柱差で流し、試料 100 μL の通過時間を測定した。通過時間は試料測定の直前に測定された生理食塩水 100 μL の通過時間を用いて（通過時間）×12 秒/（生理食塩水通過時間）により生理食塩水通過時間が 12 秒の場合に換算した。また、流動中と停止後の試料の顕微鏡写真を撮影した。

【結果】

1. 各種代用血漿剤に分散させた HbV とその血液混合系のレオロジー特性

Fig. 1A に、各種代用血漿剤に分散させた HbV について、剪断速度を 10^3 s^{-1} から 10^{-4} s^{-1} に低下させたときの粘度変化を示した。rHSA に分散させた場合（HbV-rHSA）は、粘度の変化は殆ど無く、ほぼニュートン流体を示した。HbV-rHSA および HbV-HES_{70} の粘度は、ヒト血液とほぼ同じであった。使用したレオメータの検出感度では、低粘度試料は 0.5 s^{-1} が限界であった。一方、HbV-HES_{130}、HbV-HES_{200}、HbV-HES_{670}、HbV-DEX、HbV-MFG はヒト血液よりも高い粘度を示し、高剪断速度になるほど粘度が低下する Shear-thinning 流動が観測された。この非ニュートン流体の性質は HbV の凝集体の生起に起因する。これらはより低剪断速度までの測定が可能であった。HES の分子量が大きくなるにつれ粘度が高くなる傾向が認められ、高分子量であるほど HbV は凝集し易くなることが明確に示された。

Fig. 1B に、各種代用血漿剤に分散させた HbV と血液を体積比 1：1 で混合した溶液について、**Fig. 1A** と同様に測定した結果を示した（剪断速度 10^3 – 10^{-4} s^{-1}、25 ℃）。HbV-rHSA の血液混合液は血液よりも低い粘度を示した。HbV-HES_{70}、HbV-HES_{130} の血液混合液は血液とほぼ同じ粘度を示した。一方、HbV-DEX、HbV-HES_{670}、HbV-HES_{200}、HbV-MFG の血液混合液は、混合前と比較して全域で粘度の減少を示したが、血液よりも高い粘度であった。

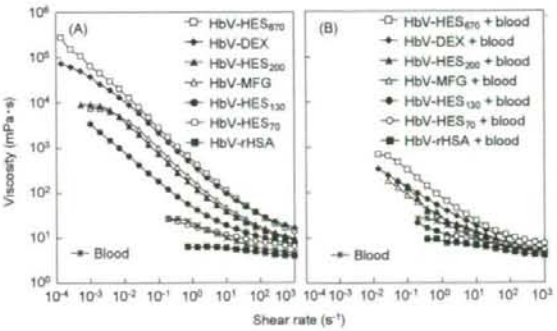

FIGURE 1. Shear rate dependence of the viscosity of **(A)** the HbV suspended in various plasma-substitute solutions ([Hb] = 10 g/dL), and **(B)** the mixtures of blood and HbV suspended in various plasma-substitute solutions at a volume ratio of 1/1. The shear rate decreased from 10^3 to 10^{-4} s^{-1} at 25°C. The blood data are inserted for comparison.

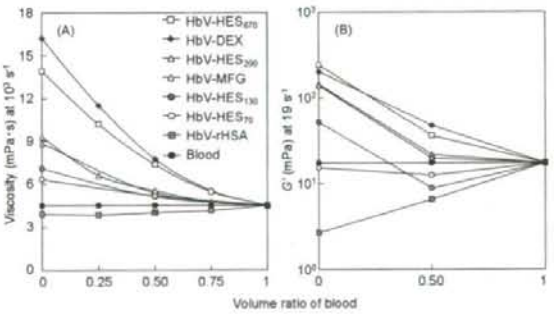

FIGURE 2. Viscoelasticity of the mixtures of blood and HbV suspended in various plasma-substitute solutions at a volume ratio of 0/1, 1/3, 1/1, 3/1, and 1/0. **(A)** The viscosity at a shear rate of 10^3 s^{-1} measured with an MCR 301 rheometer at 25°C. **(B)** The storage modulus (G') at a shear rate of 1.9 s^{-1} measured with a capillary rheometer at 37°C.

Fig. 2 には血液と HbV 分散液の混合比を変化させたときの**(A)** 粘度、**(B)** 貯蔵弾性率 G'の変化を示す。HbV-rHSA を除く HbV 分散液に関して、血液混合比の増大に伴い粘度と G'が減少する傾向が観測された。一方、HbV-rHSA の粘度と G'は血液よりも小さいため、血液混合比の増大に伴ってこれらが増大し、血液の値に収束していく傾向が観測された。

2. 各種代用血漿剤に分散させた HbV とその血液混合系のマイクロチャネル流動性試験

各種代用血漿剤に分散させた HbV とその血液混合系の流動性試験を、体積混合比を変化させて行った。全血の通過時間（46 秒）は他の文献の報告値とほぼ一致した[22]。HbV-DEX の通過時間は 196 秒であったが、血液混合比の増大に伴い通過時間は短縮し、HbV-DEX と血液の混合比 1 : 3 においては 59 秒であった。**Fig. 3** には、各種代用血漿剤に分散させた HbV と血液を体積比1 : 1 で混合した分散液の静止状態と流動状態の顕微鏡観察写真を示した。HbV の粒子径は 279 ± 95 nm と小さい為、均一分散系においてはその存在を光学顕微鏡で確認できないが、静止状態で形成される凝集体はみかけのサイズが大きい為に血漿相中に確認できた。血液と同等の粘度を示した HbV-rHSA、HbV-HES_{70} は HbV の凝集体が殆ど観測されなかった。一方、高粘度を示した HbV-HES_{670}、HbV-DEX、HbV-MFG は HbV の凝集体が観測された。しかし、流動中の凝集体は解離して流路を殆ど閉塞せずに流動した。剪断速度 1000 s^{-1}における試料の粘度とマイクロチャネルの通過時間の相関を検討したところ（**Fig. 4**）、HbV 分散液の粘度と通過時間(流量の逆数)に比例関係が成立した。直線の式を最小二乗法で求めると $Y = 12.1X$（Y：通過時間（sec/100 μL）、X：粘度（mPa・s）、$R^2 = 0.9728$）であり、Poiseuille の法則に従った。

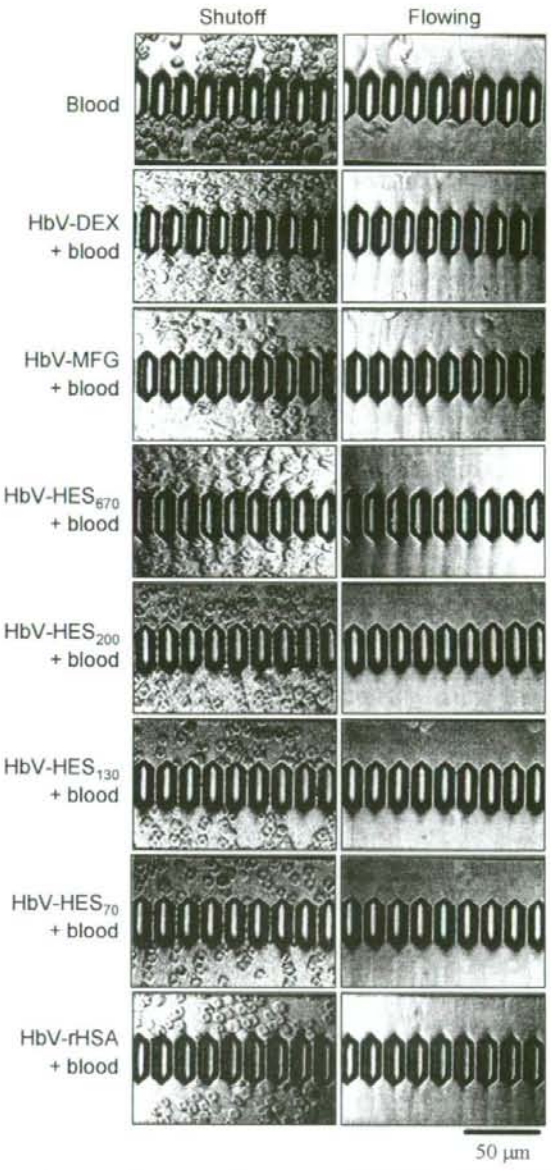

FIRURE 3. Images of microchannels during the flowing condition and the cessation of flow. The flocculate formation is apparent in the plasma phase at the cessation for HbV-DEX + blood, HbV-HES + blood, and HbV-MFG + blood. However, no flocculation was apparent for HbV-rHSA + blood. In the flowing condition, partial plugging of channels occurred due to platelets or white blood cells in blood samples (top).

【考察】

リン脂質小胞体（リポソーム）が水溶性高分子と相互作用して凝集体を形成する現象については多くの報告例があるが[23-25]、その殆どが希薄溶液の濁度または光散乱の計測で観察しているに過ぎない。HbV は、表面に修飾されたポリエチレングリコール（PEG）鎖の立体反発効果によって、血漿中においても均一な分散系を形成する[26]。しかし、HbV は極めて高濃度の分散系であるため（固形分濃度: 16 g/dL, 占有体積: 40 vol%）、これが凝集した場合は、凝集体が溶液全体に三次元ネットワークを形成し、これが固体的性質を与え、粘度及び貯蔵弾性率 G'の増大として観察されると考えられる。赤血球も可逆的な凝集体を形成し、40～45 vol%の体積を占有するので、これが血液を非ニュートン流体とする主要な因子であり、また血液に水溶性高分子が混合されると赤血球が凝集し、血液粘度、血行動態、組織酸素化に影響を及ぼすことが知られている[27-30]。従って、HbV 分散液についても同様のレオロ

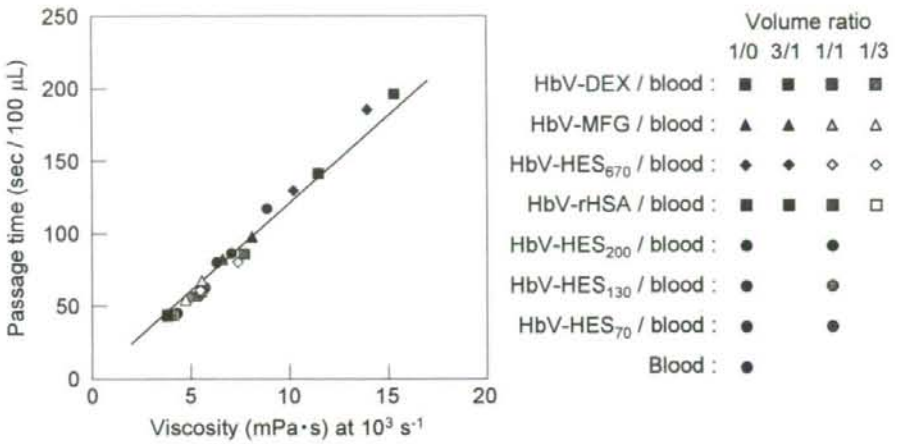

FIGURE 4. Microchannel flow measurements of the mixtures of blood and HbV suspended in various plasma-substitute solutions at a volume ratio of 1/0, 3/1, 1/1, 1/3, and 0/1. The time required for the passage of 100 μL of each suspension was plotted against the viscosity at 10^3 s^{-1}. The straight line indicates a linear approximation : $Y = 12.1X$ ($R^2 = 0.9728$).

ジー特性の解析を行った。

HbV-rHSA 分散液はほぼニュートン流体の特性を示し、高剪断速度における粘度は血液とほぼ同等であった（**Fig. 1A**）。HbV の表面に修飾された PEG 鎖がアルブミン中の分散安定度に寄与していると考えられる [3]。対照的に HES、DEX、MFG に分散させた HbV は、低剪断速度で高い粘度を示し剪断速度が高くなるに従い粘度が低下する Shear-thinning を示した（**Fig. 1A**）。これは凝集分散系に特徴的な粘度挙動である。また HES(Mw. 70, 130, 200, 670 kDa)について、凝集体形成には分子量依存性が存在し、高分子量になるほど高粘度を示した。分子量が最も小さい HES_{70} に分散させた場合には血液と同等であった。現行の PEG 修飾の条件は、血漿中での分散安定度を維持するには十分と思われる。しかし、本研究で代用血漿剤によっては PEG 修飾が施されても HbV の凝集体が形成してしまうことが明らかとなった。

リポソーム凝集の機序については、幾つかの理論が提唱されている。(i) 水溶性高分子鎖が粒子表面に吸着することにより粒子間を架橋する [24]、(ii) 水溶性高分子がリポソーム表面から水和水を奪い、リポソームが溶液から排除される [31]、また、(iii) リポソームの水和領域から高分子が排除されるため、リポソーム粒子間に形成される空間からも高分子が排除されることになり、バルク溶液とリポソーム粒子間の溶液との間に浸透圧差が生じ、この浸透圧差を小さくするために凝集が促進されて粒子間距離が短くなる [23, 32-34] と言われている。特に(iii)の場合、粒子間に形成される空間の大きさと高分子の大きさの相対的寸法差が重要と成る。HES、DEX、MFG には分岐構造があるので、球状蛋白質の rHSA に比較してより低密度で排除体積の大きい構造をしていると考えられる。DEX は水中でコイル状の分子構造をとることが報告されている [35]。MFG は、修飾されたコハク酸の静電反発によって拡大した分子構造をとる [36]。この様な高分子はリポソーム表面から排除され易く、リポソーム凝集が促進されると考えられる。また、(i)の機序でも、直鎖状構造の高分子が粒子間を架橋し易いと考えられる。一方、HES の分子構造は分岐状であり [37]、その形は球状に近いので、排除体積は DEX、MFG と比較して小さいと考えられる。しかし、高分子量体になるに従い、排除体積も大きくなるので、リポソーム凝集が促進される。我々は各種代用血漿剤に含まれる水溶性高分子の慣性半径の違いから凝集度を説明できると考えており、現在その解析を進めている。また、水溶性高分子による凝集を抑制する為に、現行よりも鎖長の長い PEG 鎖を HbV 表面に修飾し、粒子間の立体反発力を高めることも可能と考えられる。事実、我々はリポソームの表面に修飾する PEG 鎖の分子量を大きくさせると、リポソームの分散安定性が増加することを報告している [38]。

実際に HbV の投与を行う場合には、①代用血漿剤を投与した後に生理食塩水に分散された HbV を投与、或いは②濃厚な代用血漿剤（例：25%アルブミン溶液）があればこれを HbV 分散液に添加して同時に投与（[Hb] = 8.6 g/dL）するなどが想定される。血液交換率は 50%程度と想定され、HbV、代用血漿剤ともに更に希釈されるので凝集は低減されると考えられる。事実、DEX、HES_{670}、MFG に分散させた HbV は血液よりも

高い粘度を示したが、血液と体積比1:1で混合すると全ての剪断速度で粘度が減少した（**Fig. 1B**）。更に血液の混合比の増大に伴い、粘度およびG'が減少する傾向が観測された（**Fig. 2**）。HbVと代用血漿剤の双方が血液で希釈され、凝集の低減が起きることが明らかとなった。

次に、各種代用血漿剤に分散させたHbVと血液の混合系がマイクロチャネルを流動する挙動をMC-FANを用いて検討した。血液のマイクロチャネルの通過時間は、赤血球の変形能[39]、白血球による流路の塞栓[40]および血栓による塞栓[41]などが影響すると考えられる。このうち、赤血球の変形能はレオメータでの粘度測定にも影響を及ぼすが[39]、流路の塞栓はマイクロチャネルを持つMC-FANでしか測定できない項目である。我々は各種代用血漿剤に分散させたHbVがマイクロチャネルを一切塞栓することなく流動し、100 μLの通過時間と粘度に比例関係が得られ、これがPoiseuillesの法則に従っていることを報告してきた[8]。この関係が成り立つのは流路の塞栓が無い場合に限られる。仮に流路の塞栓が顕著であれば、通過時間は大きく延長して、粘度との比例関係は成立しない筈である。結果より、各種代用血漿剤に分散させたHbVと血液の混合液の通過時間は、全例が粘度に比例した（**Fig. 4**）。よって各種代用血漿剤に分散させたHbVは血液の流路塞栓因子に影響を及ぼさないと考えられる。事実、我々はラットを用いた60 %血液交換試験において、各種代用血漿剤を投与後、HbVによる蘇生を行ったが、凝集体による影響は全く見られず、全例が生存した[42]。この理由として、代用血漿剤、血液、HbVが互いに希釈され、凝集が低減したこと、凝集体が血液の剪断速度に応じて可逆的に形成・解離したこと、そして血液中の塞栓因子に影響が無かったことなどが考えられる。

最近、幾つかの研究グループが、高粘性流体が血管壁に対し、より高い剪断応力を与えるため血管拡張分子を誘導させ結果的に末梢血流が改善されると主張している[43,44]。EmiらはHbVをHES_{200}あるいはDEX (Mw 70 kDa)に分散させ、ハムスターの循環血液量の40%を交換し、毛細血管の塞栓が無いことを確認し、むしろ有茎皮弁の虚血領域の微小循環を改善する効果があることを見出した[12-14]。高粘性流体では末梢毛細管により均一に圧力が伝播し、血液をより均一に輸送し、有効毛細管密度(Functional Capillary Density)の向上が期待できる[45]。この点に関しては、HbVは代用血漿剤の併用によって特徴的なレオロジー特性を示し、またその調節も可能であるので、輸血代替以外の臨床応用にも利用できる可能性がある。今後は、HbVと一連の代用血漿剤を併用したときの安全性について詳細を確認するとともに、凝集の機序を明らかにして行く計画である。

【結論】

HbVを各種代用血漿剤に分散させた溶液と血液の混合系に関して、レオロジー特性および凝集の可逆性について検討した。$HES_{70,130}$、rHSAに分散させたHbVと血液の混合液の粘度は血液と同等もしくはそれ以下であった。DEX、高分子量HES、MFGではHbVは凝集するが、血液中においても外力に依存して瞬時に解離すると共に、血液混合比の増大に伴い凝集の形成は低減することが確認された。HbV分散液と血液の混合系のマイクロチャネルの通過時間は単純に粘度に比例し、流路の塞栓は殆ど無かったことからHbV凝集体は血液の流路の塞栓因子に影響を与えないと考えられた。凝集体生起の生体への影響を確認する必要があるが、HbV分散液は分散媒との組み合わせでレオロジー特性を調節することができるので、輸血代替以外の用途に拡大する可能性もある。

【謝辞】

代用血漿剤の生理的作用に関し、高折益彦名誉教授（東宝塚さとう病院）、Dr. Amy G. Tsai（Univ. of California, San Diego）およびProf. Dominique Erni（Inselspital Hospital, Univ. of Bern）の助言を得た。また粘弾性計測に関し、大坪泰文教授（千葉大学工学部）および平野尚也氏（日本シーベルヘグナー社）より助言を得た。使用した代用血漿剤のうち、rHSA、$HES_{130,200}$、およびMFGはそれぞれ、ニプロ社、Fresenius社、およびB. Braun社より頂戴した。記して謝意を表する。本研究は、厚生労働科学研究費補助金（医薬品・医療機器等レギュラトリーサイエンス総合研究事業）により推進された。

【文献】

1) Torchilin VP. Recent advances with liposomes as pharmaceutical carriers. *Nat. Rev. Drug Discovery*, 2005; 4: 145-160.
2) Izumi Y, Sakai H, Hamada K, Takeoka S, Yamahata T, Kato R, Nishide H, Tsuchida E, and Kobayashi K. Physiologic responses to exchange transfusion with hemoglobin vesicles as an artificial oxygen carrier in anesthetized rats: Changes in mean arterial pressure and renal cortical tissue oxygen tension. *Crit. Care Med.*, 1996; 24: 1869-1873.
3) Sakai H, Takeoka S, Park SI, Kose T, Nishide H, Izumi Y, Yoshizu A, Kobayashi K, and Tsuchida E. Surface modification of hemoglobin vesicles with poly(ethylene glycol) and effects on aggregation,

viscosity, and blood flow during 90 % exchange transfusion in anesthetized rats. *Bioconjugate Chem.*, 1997; 8: 23-30.

4) Chang TM, Hemoglobin-based red blood cell substitutes. *Artif. Organs*, 2004; 28: 789-794.
5) Phillips WT, Klipper, RW, Awasthi VD, Rudolph AS, Cliff R, Kwasiborski V, Goins BA. Polyethylene glycol-modified liposome-encapsulated hemoglobin: A long circulating red cell substitute *J. Pharmacol. Exp. Ther.*, 1999; 288: 665-670.
6) Sakai H, Hamada K, Takeoka S, Nishide H, and Tsuchida E. Physical properties of hemoglobin vesicles as red cell substitutes. *Biotechnol. Prog.*, 1996; 12: 119-125.
7) Sakai H, Horinouchi H, Yamamoto M, Ikeda E, Takeoka S, Takaori M, Tsuchida E, and Kobayashi K. Acute 40 percent exchange-transfusion with hemoglobin-vesicles (HbV) suspended in recombinant human serum albumin solution: degradation of HbV and erythropoiesis in a rat spleen for 2 weeks. *Transfusion*, 2006; 46: 339-347.
8) Sakai H, Sato A, Takeoka S, and Tsuchida E. Rheologial properties of hemoglobin vesicles (artificial oxygen carriers) suspended in a series of plasma-substitute solutions. *Langmuir*, 2007; 23: 8121-8128.
9) Webb AR, Nash GB, Dormandy JA, and Bennett ED. A comparison of the effects of artificial plasma substitutes, albumin and saline solutions on in vitro apparent blood viscosity. *Clin. Hemorheol.*, 1990; 10: 287-296
10) Webb AR, Barclay SA, and Bennett ED. In vitro colloid osmotic pressure of commonly used plasma expanders and substitutes: a study of the diffusibility of colloid molecules. *Intensive Care Med.*, 1989; 15: 116-120.
11) Traylor RJ and Pearl RG. Crystalloid versus colloid versus colloid: all colloids are not created equal. *Anesth. Analg.*, 1996; 83: 209-212.
12) Plock JA., Contaldo C, Sakai H, Tsuchida E, Leunig M, Banic A, Menger MD, and Erni D. Is hemoglobin in hemoglobin vesicles infused for isovolemic hemodilution necessary to improve oxygenation in critically ischemic hamster skin? *Am. J. Physiol. Heart Circ. Physiol.*, 2005; 289: H2624-H2631.
13) Contaldo C, Schramm S, Wettstein R, Sakai H, Takeoka S, Tsuchida E, Leunig M, Banic A, and Erni D. Improved oxygenation in ischemic hamster flap tissue is correlated with increasing hemodilution with Hb vesicles and their O_2 affinity. *Am. J. Physiol. Heart Circ. Physiol.*, 2003; 285: H1140-H1147.
14) Contaldo C, Plock J, Sakai H, Takeoka S, Tsuchida E, Leunig M, Banic A, and Erni D. New generation of hemoglobin-based oxygen carriers evaluated for oxygenation of critically ischemic hamster flap tissue. *Crit. Care Med.*, 2005; 33: 806-812.
15) Kikuchi Y, Sato K, Ohki H, and Kaneko T. Optically accessible microchannels formed in a single-crystal silicon substrate for studies of blood rheology. *Microvasc. Res.*, 1992; 44: 226-240.
16) Kikuchi Y, Sato K, and Mizuguchi Y. Modified cell-flow microchannels in a single-crystal silicon substrate and flow behavior of blood cells. *Microvasc. Res.*, 1994; 47: 222-231.
17) Sakai H, Takeoka S, Yokohama H, Seino Y, Nishide H, and Tsuchida E. Purification of concentrated Hb using organic solvent and heat treatment. *Protein Expression Purif.*, 1993; 4: 563-569.
18) Sakai H, Yuasa M, Onuma H, Takeoka S, and Tsuchida E. Synthesis and physicochemical characterization of a series of hemoglobin-based oxygen carriers: objective comparison between cellular and acellular types. *Bioconjugate Chem.*, 2000; 11: 56-64.
19) Sou K, Naito Y, Endo T, Takeoka S, and Tsuchida E. Effective encapsulation of proteins into size-controlled phospholipid vesicles using freeze-thawing and extrusion. *Biotechnol. Progr.*, 2003; 19: 1547-1552.
20) Sakai H, Tomiyama K, Sou K, Takeoka S, and Tsuchida E. Poly(ethylene glycol)-conjugation and deoxygenation enable long-term preservation of hemoglobin-vesicles as oxygen carriers in a liquid state. *Bioconjugate Chem.*, 2000; 11: 425-432.
21) 関 耕二, 角野 博之, 村上 正巳. MC-FAN を用いて測定した血液流動性について. *臨床病理*, 2003; 51: 770-775.
22) 菊池 佑二, 高橋 千栄子, 磯野 厚子. 健常者の部分母集団における MC-FAN 全血通過時間の分布. *ヘモレオロジー研究会誌*, 2001; 4: 7-14.
23) Meyuhas D, Nir S, and Lichtenberg D. Aggregation of phospholipid vesicles by water-soluble polymers. *Biophys. J.*, 1996; 71: 2602-2612.
24) Sunamoto J, Iwamoto K, and Kondo H. Liposomal membranes. VII. Fusion and aggregation of egg lecithin liposomes as promoted by polysaccharides. *Biochem. Biophys. Res. Commun.*, 1980; 94: 1367-1373.

25) Sou K, Endo T, Takeoka S, and Tsuchida E. Poly(ethylene glycol)-modification of the phospholipid vesicles by using the spontaneous incorporation of poly(ethylene glycol)-lipid into the vesicles. *Bioconjugate Chem.*, 2000; 11: 372-379.

26) Sakai H, Tsai AG, Kerger H, Park SI, Takeoka S, Nishide H, Tsuchida E, and Intaglietta M. Subcutaneous microvascular responses to hemodilution with a red cell substitute consisting of polyethyleneglycol-modified vesicles encapsulating hemoglobin. *J. Biomed. Mater. Res.*, 1998; 40: 66-78.

27) Freyburger G, Dubreuil M, Boisseau MR, and Janvier G. Rheological properties of commonly used plasma substitutes during preoperative normovolaemic acute haemodilution. *Br. J. Anaesth.*, 1996; 76: 519-525.

28) Eckmann DM, Bowers S, Stecker M, and Cheung AT. Hematocrit, volume expander, temperature, and shear rate effects on blood viscosity. *Anesth. Analg.*, 2000; 91: 539-545.

29) Bishop JJ, Nance PR, Popel AS, Intaglietta M, and Johnson PC. Effect of erythrocyte aggregation on velocity profiles in venules. *Am. J. Physiol. Heart Circ. Physiol.*, 2001; 280: H222-H236.

30) Tateishi N, Suzuki Y, Cicha I, and Maeda N. O_2 release from erythrocytes flowing in a narrow O_2-permeable tube: effects of erythrocyte aggregation. *Am. J. Physiol. Heart Circ. Physiol.*, 2001; 281: H448-H456.

31) Tilcock CP and Fisher D. The interaction of phospholipid membranes with poly(ethylene glycol). Vesicle aggregation and lipid exchange. *Biochim. Biophys. Acta*, 1982; 688: 645-652.

32) Neu B and Meiselman HJ. Depletion-mediated red blood cell aggregation in polymer solutions. *Biophys. J.*, 2002; 83: 2482-2490.

33) Neu B and Meiselman HJ. Depletion interactions in polymer solutions promote red blood cell adhesion to albumin-coated surfaces. *Biochim. Biophys. Acta*, 2006; 1760: 1772-1779.

34) Vincent B, Edwards J, Emmett S, and Jones A. Depletion flocculation in dispersions of sterically-stabilised particles ("soft spheres"). *Colloids Surf.*, 1986; 18: 261-281.

35) Hirata Y, Sano Y, Aoki M, Shohji H, Katoh S, Abe J, Hitsukuri S, and Yamamoto H. Small-angle X-ray scattering studies of moderately concentrated dextran solution. *Carbohydr. Polym.*, 2003; 53: 331-335.

36) Saddler JM, and Horsey PJ. The new generation gelatins. *Anaesthesia*, 1987; 42: 998-1004.

37) Gosch CI, Haase T, Wolf BA, and Kulicke WM. Molar mass distribution and size of hydroxyethyl starch fractions obtained by continuous polymer fractionation. *Starch*, 2002; 54: 375-384.

38) Takeoka S, Mori K, Ohkawa H, Sou K, and Tsuchida E. Synthesis and assembly of poly (ethylene glycol)-lipids with mono-, di-, and tetraacyl chains and a poly (ethylene glycol) chain of various molecular weights. *J. Am. Chem. Soc.*, 2000; 122: 7927-7935.

39) Lee CYJ, Kim KC, Park HW, Song JH, and Lee CH. Rheological properties of erythrocytes from male hypercholesterolemia. *Microvasc. Res.*, 2004; 67: 133-138.

40) Miyamoto K, Ogura Y, Kenmochi S, and Honda Y. Role of leukocytes in diabetic microcirculatory disturbances. *Microvasc. Res.*, 1997; 54: 43-48.

41) Kamada H, Hattori K, Hayashi T, Suzuki K. In vitro evaluation of blood coagulation activation and microthrombus formation by a microchannel array flow analyzer. *Thromb. Res.*, 2004; 114: 195-203.

42) 酒井 宏水, 佐藤 敦, 宮川 賀仁, 武岡 真司, 堀之内 宏久, 高折 益彦, 小林 紘一, 土田 英俊. ヘモグロビン小胞体と各種代用血漿剤の併用に関する検討. *人工血液*, 2007; 15: 23.

43) Cabrales P, Tsai AG, and Intaglietta M. Alginate plasma expander maintains perfusion and plasma viscosity during extreme hemodilution. *Am. J. Physiol. Heart Circ. Physiol.*, 2005; 288: H1708-H1716.

44) Cabrales P, Intaglietta M. and Tsai AG. Increase plasma viscosity sustains microcirculation after resuscitation from hemorrhagic shock and continuous bleeding. *Shock*, 2005; 23: 549-555.

45) Tsai AG, Friesenecker B, McCarthy M, Sakai H, and Intaglietta M. Plasma viscosity regulates capillary perfusion during extreme hemodilution in hamster skin fold model. *Am. J. Physiol. Heart Circ. Physiol.*, 1998; 275: H2170-2180.

Rheological properties of hemoglobin-vesicles (artificial red cells) suspended in a series of plasma-substitute solutions and their mixtures with blood.

Atsushi Sato[1], Hiromi Sakai[2], Shinji Takeoka[1], and Eishun Tsuchida[2]
[1] Graduate School of Science and Engineering, Waseda University
[2] Research Institute for Science and Engineering, Waseda University

【ABSTRACT】

Hemoglobin-vesicles (HbV) are artificial oxygen carriers. The HbV suspension has an oxygen-carrying capacity that is comparable to that of blood. Since HbV suspension does not possess a colloid osmotic pressure, it should be suspended in or co-injected with an aqueous solution of a plasma substitute (water-soluble polymer), which might interact with HbV. This article describes the rheological properties of HbV suspended in a series of plasma substitute solutions and their mixtures with human blood. HbV suspended in a recombinant human serum albumin solution was nearly Newtonian and that mixtures with blood exhibited very low viscoelasticity. On the other hand, HbV suspended in a solution of dextran, modified fluid gelatin, or high-molecular-weight hydroxyethyl starch exhibited higher viscoelasticity. However, it decreased with increasing the volume ratio of blood. Microscopically, the flow pattern of the mixture of blood and flocculated HbV perfused through microchannels (4.5 μm wide, 20 cmH_2O applied pressure) showed few plugging. Furthermore, the time required for passing was simply proportional to the viscosity. This result indicates that flocculated HbVs would not affect the plugging factor of blood when perfusing through microchannels. The HbV suspension would be useful as various clinical applications in addition to its use as a transfusion alternative by manipulating the rheological property.

THE JOURNAL OF BIOLOGICAL CHEMISTRY VOL. 283, NO. 3, pp. 1508–1517, January 18, 2008

Encapsulation of Concentrated Hemoglobin Solution in Phospholipid Vesicles Retards the Reaction with NO, but Not CO, by Intracellular Diffusion Barrier*

Received for publication, September 12, 2007, and in revised form, November 13, 2007 Published, JBC Papers in Press, November 14, 2007, DOI 10.1074/jbc.M707660200

Hiromi Sakai[‡], **Atsushi Sato**[§], **Kaoru Masuda**[¶], **Shinji Takeoka**[§¶], **and Eishun Tsuchida**[‡2]

From the [‡]*Research Institute for Science and Engineering and* [§]*Graduate School of Advanced Science and Engineering, Waseda University, Tokyo 169-8555, Japan and* [¶]*Kobelco Research Institute, Inc., Kobe 651-2271, Japan*

One physiological significance of the red blood cell (RBC) structure is that NO binding of Hb is retarded by encapsulation with the cell membrane. To clarify the mechanism, we analyzed Hb-vesicles (HbVs) with different intracellular Hb concentrations, $[Hb]_{in}$, and different particle sizes using stopped-flow spectrophotometry. The apparent NO binding rate constant, $k'_{on}{}^{(NO)}$, of HbV at $[Hb]_{in}$ = 1 g/dl was 2.6×10^7 M^{-1} s^{-1}, which was almost equal to $k_{on}{}^{(NO)}$ of molecular Hb, indicating that the lipid membrane presents no obstacle for NO binding. With increasing $[Hb]_{in}$ to 35 g/dl, $k'_{on}{}^{(NO)}$ decreased to 0.9×10^7 M^{-1} s^{-1}, which was further decreased to 0.5×10^7 M^{-1} s^{-1} with enlarging particle diameter from 265 to 452 nm. For CO binding, which is intrinsically much slower than NO binding, $k'_{on}{}^{(CO)}$ did not change greatly with $[Hb]_{in}$ and the particle diameter. Results obtained using diffusion simulations coupled with elementary binding reactions concur with these tendencies and clarify that NO is trapped rapidly by Hb from the interior surface region to the core of HbV at a high $[Hb]_{in}$, retarding NO diffusion toward the core of HbV. In contrast, slow CO binding allows time for further CO-diffusion to the core. Simulations extrapolated to larger particles (8 μm) showing retardation even for CO binding. The obtained $k'_{on}{}^{(NO)}$ and $k'_{on}{}^{(CO)}$ yield values similar to those reported for RBCs. In summary, the intracellular, not extracellular, diffusion barrier is predominant due to the rapid NO binding that induces a rapid sink of NO from the interior surface to the core, retarding further NO diffusion and binding.

Physicochemical analyses of O_2 uptake and release behaviors of red blood cells (RBCs)[3] have revealed that the cellular structure retards all reactions in comparison with the homogeneous cell-free Hb solution (1–5). However, nature has selected this cellular structure through evolution. Reasons for Hb encapsulation in RBCs are as follows: (i) decreases in a high colloidal osmotic pressure of an Hb solution; (ii) prevention of removal of Hb from blood circulation through renal gloreruli; (iii) preservation of the chemical environment in cells, such as the concentrations of electrolytes (phosphates, 2,3-diphosphoglyceric acid, ATP, etc.) and many enzymes; and (iv) modulation of entrapment of endogenous gaseous messenger molecules (NO and CO) (6, 7) because it has been clarified in pathological conditions with hemolysis (8) and in the development of some Hb-based oxygen carriers (HBOCs) (9–16) that entrapment of endothelium-derived NO induces vasoconstriction, hypertension, reduced blood flow, and vascular damage. CO is also a vasorelaxation factor, especially in hepatic microcirculation (17). Entrapment of CO by a cell-free Hb solution induces constriction of sinusoidal capillaries (18). These side effects of molecular Hb imply the importance of the cellular structure of RBC.

Despite such a background in this field, the mechanism of retardation of NO binding by Hb encapsulation in RBC remains controversial (19–21). It remains unclear whether (i) an unstirred layer is formed as an extracellular diffusion barrier surrounding the RBC (6, 9); (ii) a protein-rich RBC cytoskeletal submembrane becomes a physical barrier against NO diffusion (22, 23); or (iii) gas diffusion is retarded because of the viscous Hb solution in RBC (2). As chemists, it seems to us that these controversies are attributable to the complex and fragile structure of RBC and chemically unstable NO, which make it difficult to analyze the binding rate constant of NO to RBC.

Hemoglobin-vesicles (HbVs) or liposome- encapsulated Hbs have been developed as transfusion alternatives. Their efficacy as O_2 carriers is comparable with that of RBC (24–28). It has been thought that liposomes as a molecular assembly are a fragile capsule. However, appropriate lipid composition and polyethylene glycol modification on the surface of vesicles stabilize the dispersion state (29) and enable stopped-flow measure-

* This work was supported in part by Health and Labor Sciences Research Grants (Research on Regulatory Science of Pharmaceuticals and Medical Devices), Ministry of Health, Labor, and Welfare, Japan (to H. S. and E. T.) and by Grants-in-Aid for Scientific Research from the Japan Society for the Promotion of Science 816300162 (to H. S.) and 18500368 (to S. T.), and Global COE "Practical Chemical Wisdom" (to S. T.). The costs of publication of this article were defrayed in part by the payment of page charges. This article must therefore be hereby marked "*advertisement*" in accordance with 18 U.S.C. Section 1734 solely to indicate this fact.

[1] Present address: Consolidated Research Institute for Advanced Science and Medical Care, Waseda University, 3-4-1 Okubo, Shinjuku, Tokyo 169-8555, Japan.

[2] To whom correspondence should be addressed: Research Institute for Science and Engineering, Waseda University, 3-4-1 Okubo, Shinjuku, Tokyo 169-8555, Japan. Tel.: 81-3-5286-3120; Fax: 81-3-3205-4740; E-mail: eishun@waseda.jp.

[3] The abbreviations used are: RBC, red blood cell; Hb, hemoglobin; metHb, methemoglobin; deoxyHb, deoxyhemoglobin; HbV, hemoglobin-vesicles; $[Hb]_{in}$, intracellular Hb concentration; $[heme]_{in}$, intracellular heme concentration; k_{on}, binding rate constant of elementary reaction; $k'_{on}{}^{(NO)}$, apparent NO binding rate constant; $k'_{on}{}^{(CO)}$, apparent CO binding rate constant; HBOC, Hb-based oxygen carrier; P_{50}, oxygen partial pressure at which Hb is half-saturated; D_{Hb}, diffusion constant of Hb; D_{O_2}, diffusion constant of O_2; D_{NO}, diffusion constant of NO; D_{CO}, diffusion constant of CO.

ments without causing hemolysis (26, 30). Although stopped-flow measurement is becoming classical, it allows accurate measurement of the binding rate constant of ligands (31). HbV is a molecular assembly composed of lipids and a concentrated Hb solution (32), and its physicochemical properties can be regulated easily (33–35) to elucidate their influences on the ligand binding profiles. In this paper, we describe analyses of the influences of intracellular Hb concentration, $[Hb]_{in}$, and the particle size of HbV on the apparent binding rate constants of NO and CO. Moreover, we attempted computer simulations to recreate the phenomena, clarify the underlying mechanism, and predict the ligand binding profiles of larger particles, such as RBCs.

TABLE 1

Physicochemical characterization of a series of HbV prepared for the stopped flow spectrophotometry to observe the NO and CO binding profiles

Samples 1–4 were used to examine the influence of intracellular Hb concentration ($[Hb]_{in}$). Samples 4–6 were used to study the influence of particle diameter. The P_{50} value (oxygen tension at which Hb is half-saturated with oxygen) were regulated in the narrow range of 13–16 torrs to minimize the influence of Hb allostery on the binding rate constants of NO and CO.

Sample entry number	$[Hb]_{in}$	Particle size	P_{50}
	g/dl	*nm*	*torrs*
1	1	305 ± 105	13
2	10	277 ± 103	15
3	20	278 ± 94	15
4	35	265 ± 57	14
5	35	178 ± 74	16
6	35	452 ± 184	14

EXPERIMENTAL PROCEDURES

Preparation of Hb Solution and Hb-vesicles with Various $[Hb]_{in}$—A concentrated human carbonylhemoglobin solution (40 g/dl, desalted) was obtained through purification from outdated donated blood provided by the Japanese Red Cross Society (Tokyo, Japan), as reported previously (36, 37). This was diluted by 10 times with a phosphate-buffered saline (PBS) solution (pH 7.4; Wako Pure Chemical Industries Ltd., Tokyo). It was then concentrated again to 40 g/dl using an ultrafiltration (cut-off M_r 10,000; Advantec, Tokyo) at 4 °C. This solution was diluted to 1, 10, 20, and 35 g/dl using the same PBS solution. They were used for preparation of HbV with different $[Hb]_{in}$. The viscosities of these Hb solutions were measured using a rheometer (Physica MCR 301; Anton Paar GmbH, Graz, Austria) as 0.9, 1.1, 2.1, and 10.1 centipose, respectively, at 10 s^{-1} and 25 °C. In this experiment, we added no allosteric effector, such as an organic phosphate, because we intended to compare the Hb solution and HbV with different $[Hb]_{in}$ at the same O_2 affinity (P_{50}, oxygen partial pressure at which Hb is half-saturated). A linear relationship exists between P_{50} and NO affinity of Hb (38). In the present study, P_{50} was regulated solely using Cl^- and phosphate of PBS (35). The lipid bilayer comprised 1,2-dipalmitoyl-*sn*-glycero-3-phosphatidylcholine, cholesterol, 1,5-*O*-dihexadecyl-*N*-succinyl-L-glutamate (Nippon Fine Chemical Co. Ltd., Osaka, Japan), and 1,2-distearoyl-*sn*-glycerol-3-phosphatidylethanolamine-*N*-polyethylene glycol 5000 (NOF Corp., Tokyo, Japan) at a molar composition of 5/5/1/0.033. It is reported that unsaturated phospholipids are susceptible to lipid peroxidation and induce Hb denaturation (39, 40). Hb interacts with such a liposomal membrane and converts to metHb, leading synergistically to the heme loss and lipid peroxidation. Unsaturated fatty acid is susceptible to nitration (41). However, we use saturated phospholipids that essentially do not induce such reactions (39, 40, 42). The mean particle diameter was regulated by an extrusion method to 265–305 nm to study the influence of $[Hb]_{in}$, and to 178, 265, and 452 nm at the same $[Hb]_{in}$ (equal to 35 g/dl) to study the influence of the particle diameter (32, 34, 43, 44) (Table 1). After removing the unencapsulated Hb solution using ultracentrifugation, HbV was resuspended in the same PBS solution (pH 7.4) at [heme] = 300 μM. Therefore, the carbonylhemoglobin in HbV is converted to HbO_2 by photodissociation of CO by illuminating visible light under O_2 atmosphere. Briefly, an aliquot of CO-bound HbV was put in a glass flask; this was rotated using a rotary evaporator while the flask was immersed in cold water and illuminated using a halogen lamp (500 watts) with a continuous and gentle O_2 flow inside the flask for several minutes. The complete conversion to HbO_2 was confirmed by absorption spectroscopy in the *Q* band. The physicochemical characteristics of the obtained HbVs are listed in Table 1. The particle size distribution was measured using a dynamic light-scattering method (Submicron Particle Size Analyzer, model N4 PLUS; Beckman-Coulter, Inc., Fullerton, CA). The P_{50} values were obtained from the oxygen equilibrium curve measured with a Hemox-Analyzer (TCS Medical Science, Philadelphia, PA); all samples were ~13–16 torrs at 37 °C.

Stopped-flow Analyses—The time course of the ligand binding was analyzed at a rapid mixing of a deoxygenated HbV solution and a NO-containing or CO-containing solution using a stopped-flow rapid scan spectrophotometer (model RSP-1000; Unisoku Co. Ltd., Osaka, Japan). Solutions in the two reservoirs (A and B) are mixed rapidly with an applied pressure of 0.3–0.6 megapascals and a dead time for mixing of <1.5 ms. All measurements were performed at 25 °C. A PBS solution (3 ml each) was poured into both reservoirs and sealed using septum rubber seals. The reservoirs were deoxygenated by N_2 bubbling for over 30 min for the complete removal of O_2. This is important in the case of NO bubbling to prevent the NO loss and metHb formation. The HbV stock solution (~30 μl, [heme] = 300 μM) was injected into Reservoir A to adjust [heme] finally to 3 μM; the N_2 bubbling was changed to flowing to avoid denaturation of the solutes. Complete deoxygenation was confirmed using preliminary stopped-flow measurements (wavelength: 385–593 nm), where the Soret band showed a maximum absorption (λ_{max}) at 430 nm attributable to the presence of deoxyHb. In Reservoir B, NO or CO gas bubbling was started; a gentle N_2 flowing was maintained in Reservoir A. The mixed gases for NO binding (NO, 0.2029%; N_2, 99.7971%) and for CO binding (CO, 14.14%; N_2, 85.86%) were purchased from Takachiho Chemical Industrial Co., Ltd. (Tokyo). After about 10 min of bubbling, stopped flow measurement was initiated. The sampling interval and the exposure time were set as 1 ms. The measurement time was 210 ms. All measurements were performed three times, and the change of absorbance at 430 nm was plotted as a function of time. The apparent binding rate constants of NO and CO ($k'_{on}{}^{(NO)}$, and $k'_{on}{}^{(CO)}$, respectively) were calculated using Equation 1 under the assumption of homogeneous distribution

of Hb, irreversible second order reaction, and pseudo-first-order reaction when gas molecules are abundant,

$$\ln\frac{\Delta A_t}{\Delta A_0} = -k'_{on} \cdot C_{Gas} \cdot t \qquad \text{(Eq. 1)}$$

where ΔA_t represents the change of absorbance at 430 nm at time t (equal to $A_t - A_{t=\infty}$), and ΔA_0 is the absorbance at the initial time (equal to $A_{t=0} - A_{t=\infty}$). C_{Gas} is the initial gas concentration. In the case of the NO binding experiment, NO (1.9 μM) is not excessively abundant in comparison with heme concentration (1.5 μM); therefore, we calculated the apparent binding rates from the slopes of the initial phase of reactions.

Computer Simulation—We assumed that HbV is spherical and dispersed homogeneously. The gas diffusion constants are much larger than those of Hb molecule (7 nm) and HbV (250 nm) (45). Accordingly, we analyzed only gas diffusion and the formation of ligand-bound Hb in a single HbV particle. We did not consider the extracellular diffusion barrier because of the rapid mixing of small particles, and also we did not consider the gas permeability constant in the lipid bilayer, because the thickness of the lipid bilayer (~5 nm) is thin in comparison with the particle diameter. (Our results show that they would not be important parameters in our system.) To simplify the equation, the distance from the surface to the core of HbV, 125 nm, was divided by 12.5 nm into 10 units. For simulation of a larger particle, such as that with an 8000-nm diameter, 4000 nm was divided by 12.5 nm into 320 units. The first unit is located at the HbV surface and is in the concentration boundary condition. The last unit is located in the core of HbV in the closed condition. From the gas diffusion equation (Equation 2), the one-dimensional diffusion from the surface to the core of the particle can be expressed as Equation 3,

$$\frac{\partial C_{Gas}}{\partial t} = D\frac{\partial^2 C_{Gas}}{\partial x^2} \qquad \text{(Eq. 2)}$$

$$\Delta C_{Gas}(t_i, x_j) = D \cdot \left(\frac{-A_j \cdot (C_{Gas}(t_i, x_j) - C_{Gas}(t_i, x_{j-1})) + A_{j+1} \cdot (C_{Gas}(t_i, x_{j+1}) - C_{Gas}(t_i, x_j))}{V_j \cdot \Delta x}\right) \cdot \Delta t \qquad \text{(Eq. 3)}$$

where $C_{Gas}(t_i, x_j)$ represents the gas concentration at time i (t_i) in 1 unit (x_j; distance from the surface of HbV); $\Delta C_{Gas}(t_i, x_j)$ is a mass change by diffusion; A_j is the interface area of the units $j-1$ and j, and it changes with the distance from the core of HbV; Δt is the step time; V_j is the volume of the unit j; and Δx is the distance between neighboring units. A gas molecule reacts with a heme in Hb. We assumed that the reaction is irreversible. Therefore, the changes of concentrations are expressed as Equations 4 and 5 with a binding rate constant, k_{on}, of an elementary gas binding reaction.

$$\frac{dC_{heme}}{dt} = -k_{on} \cdot C_{Gas} \cdot C_{heme} \qquad \text{(Eq. 4)}$$

$$\frac{dC_{Gas}}{dt} = \frac{dC_{heme}}{dt} \qquad \text{(Eq. 5)}$$

At a step time Δt and in a step unit Δx, the changes of concentrations (ΔC_{heme}, $\Delta C'_{Gas}$) by the gas bindings are expressed as Equations 6 and 7.

$$\Delta C_{heme}(t_i, x_j) = -k_{on} \cdot C_{Gas}(t_i, x_j) \cdot C_{heme}(t_i, x_j) \cdot \Delta t \qquad \text{(Eq. 6)}$$

$$\Delta C'_{Gas}(t_i, x_j) = -k_{on} \cdot C_{Gas}(t_i, x_j) \cdot C_{heme}(t_i, x_j) \cdot \Delta t \qquad \text{(Eq. 7)}$$

At the onset of reaction by mixing two solutions in the stopped-flow apparatus, the gas diffuses into the HbV. Therefore, the initial unbound free gas concentration inside the vesicle is assumed to be zero. The initial unbound free heme concentrations of HbV are 620–21,700 μM ($[Hb]_{in}$ = 1–35 g/dl); they decrease with the reactions of gas molecules. All initial values for calculations are summarized in Table 2. The diffusion constant of the Hb molecule is concentration-dependent and decreases from 77 to 7.4 $\mu m^2 s^{-1}$ with increasing $[Hb]_{in}$ from 1 to 35 g/dl (46–48). The diffusion constants of gases are 2 orders larger than that of Hb. The diffusion constant of O_2 in Hb solutions (D_{O_2}) decreases with increasing Hb concentration. The diffusion constants of CO and NO (D_{NO} and D_{CO}, respectively) are calculated from D_{O_2} using Equation 8 (2),

$$D_x = D_{O_2} \cdot \left(\frac{32}{MW_x}\right)^{1/2} \qquad \text{(Eq. 8)}$$

where MW_x is the molecular weight of NO or CO.

One-dimensional diffusion simulation coupled with gas binding reactions was performed based on the equations given above (Equations 3, 6, and 7) according to the finite differential method using a Visual Basic Language Programming (Excel, Microsoft Corp., Japan, Tokyo) in a personal computer. Both C_{Gas} and C_{heme} at t_i were calculated using those at t_{i-1}. Both ΔC_{heme} and $\Delta C'_{Gas}$ were calculated using Equations 6 and 7. Gas molecules diffuse depending on a concentration gradient, and the obtained ΔC_{Gas} of Equation 3 was combined with $\Delta C'_{Gas}$ of Equation 7 for the next step calculation of C_{Gas}. The time interval, Δt, was set as 0.01 μs, and 10^7 steps were required to calculate the reaction profile for 100 ms in the case of HbV with a 250-nm diameter. The data were output at every 5 ms.

As the reaction proceeds, the concentration of gas in the bulk solution decreases. To reflect this, Equation 9 is used,

TABLE 2
Parameters for computer simulations for each HbV with different $[Hb]_{in}$

Parameters	Values			
Diameter (nm)	50, 100, 200, 250, 500, 1000, 2000, 8000			
[heme] in solution (μM)	1.5			
Initial [NO] in solution (μM)	1.9			
Initial [CO] in solution (μM)	67.5			
$k_{on}^{(NO)}$ ($M^{-1} s^{-1}$)	2.7×10^7			
$k_{on}^{(CO)}$ ($M^{-1} s^{-1}$)	3.4×10^5			
	1 g/dl $[Hb]_{in}$	10 g/dl $[Hb]_{in}$	20 g/dl $[Hb]_{in}$	35 g/dl $[Hb]_{in}$
$[heme]_{in}$ (μM)	620	6200	12400	21700
D_{Hb} in HbV ($\mu m^2 s^{-1}$)	77	53	29	7.4
D_{NO} in HbV ($\mu m^2 s^{-1}$)[a]	2080	1590	1160	706
D_{CO} in HbV ($\mu m^2 s^{-1}$)[a]	2150	1640	1200	731

[a] D_{NO} in saline is 2210 $\mu m^2 s^{-1}$ and D_{CO} in saline is 2290 $\mu m^2 s^{-1}$. D_{Hb} in HbV is much smaller than D_{NO} and D_{CO}. For that reason, we did not use D_{Hb} in computer simulations. Consequently, we did not consider the so-called "facilitated gas diffusion" attributable to the diffusion and dissociation of HbNO or HbCO because of the low D_{Hb} and the significantly large equilibrium constants of HbNO and HbCO in comparison with that of HbO_2.